2019 – 2020
AIAA Design, Build, Fly

DESIGN, BUILD, FLY at the UNIVERSITY OF WASHINGTON

BOEING

ELECTROIMPACT

WILLIAM E. BOEING
DEPARTMENT OF AERONAUTICS & ASTRONAUTICS

UNIVERSITY *of* WASHINGTON

UNIVERSITY *of* WASHINGTON

Table of Contents

ACRONYMS AND NOMENCLATURE

- **ABS:** Acrylonitrile butadiene styrene
- **AC:** Alternating Current
- **AIAA:** American Institute of Aeronautics and Astronautics
- **AOA:** Angle of Attack
- **APC:** APC Propeller Company
- **Batt:** Battery
- **BB:** Ball Bearing
- **CAD:** Computer Aided Design
- **CD**: Coefficient of Drag
- **CL**: Coefficient of Lift
- **CFD:** Computational Fluid Dynamics
- **CG:** Center of Gravity
- **CNC:** Computer Numerical Control
- **Config:** Configuration
- **DBF:** Design Build Fly
- **DC:** Direct Current
- **ESC:** Electronic Speed Controller
- **FEA:** Finite Element Analysis

- **GM:** Ground Mission
- **HXT:** Hexatronik
- **i**: Angle of incidence
- **I**: Current
- **LiPo:** Lithium-Polymer (often refers to batteries)
- **m**: Mass
- **M1:** Flight Mission 1
- **M2:** Flight Mission 2
- **M3:** Flight Mission 3
- **PLA:** Polylactic Acid
- **Ply:** Plywood
- **RPM:** Revolutions per Minute
- **Rx:** Receiver
- **TGY**: Turnigy
- **UW:** University of Washington
- **v**: Velocity
- **W**: Weight
- **XPS:** Extruded polystyrene

1. Executive Summary

This report details the design, manufacturing and testing of the *Phoenix*, the aircraft entered by the Design Build Fly team at the University of Washington in the 2020 AIAA Design Build Fly (DBF) competition. The aircraft was designed to complete the following tasks: an empty flight, a flight carrying a complete load of passengers and luggage, and a flight where the banner would be remotely deployed, flown while extended, and subsequently released. The first and third flight missions also need to be completed with a takeoff distance of 20 ft or less, which required that the plane be designed for short takeoff. In addition, a ground mission that tested the structural capabilities of the aircraft and the accessibility of the passengers would need to be completed prior to the flight missions. The aircraft was not permitted to have a wingspan exceeding five feet, and energy utilized for propulsion must be 200 Watt-hours or less.

Based on data from past competitions, the *Phoenix* was designed and manufactured to excel at all mission requirements. Based on the mission objectives, a conceptual list of systems and subsystems was created and analyzed based on several key parameters, including effectiveness, cost, ease of manufacturing, and reliability. From this analysis, a preliminary aircraft configuration was developed and calculations for prototypical structures and systems were conducted. This preliminary design was then optimized based on calculations, computational analysis, and field tests, until a final aircraft configuration was reached. From this configuration, the dimensions of the aircraft and the components were finalized, manufactured, and tested.

The aircraft is powered by two batteries that fit within the 200 Watt-hour requirement, and utilizes two motors, one mounted on each wing, as a source of propulsion. The passengers would be housed inside a tray designed such that movement in any direction would be impossible under stable flight conditions. A banner housing and deployment mechanism attached to a large vertical stabilizer would hold the banner, while an avionics package that utilized servo motors would control its deployment and release. All of these systems, as well as the overall aircraft, fit all design parameters. The passenger tray has held up to 24 passengers and luggage, while the banner mechanism has supported banners of several lengths. The performance of the aircraft with these mission systems was tested both statically and in the air, and test missions were successfully completed.

2. Management Summary

The team at the University of Washington consists of 69 members, the majority of whom were freshman new to the university, as shown in Figure 2.1. The team was led by seven lead members, all of whom had previous competition experience. The objective of the team was for experienced junior and senior members to educate young team members, allowing them to gain experience with all aspects of large-scale engineering projects via the AIAA DBF competition.
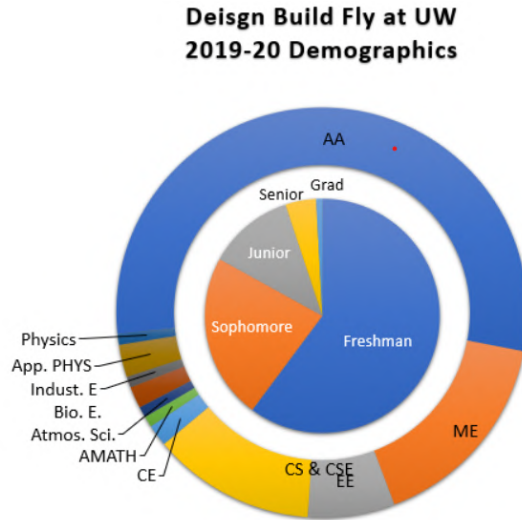

Figure 2.1: Demographics of the team

2.1 Team Organization

The team was entirely student-led, with only ten students having prior competition experience. A team of seven students made up the leadership team, and were responsible for seven sub-teams, each of which was responsible for overseeing individual projects and ensuring that work was completed on time and to a high standard. Each sub-team also had a number of project leads, each responsible for a specific project such as motor mount, passenger storage, and landing gear. Four of the teams were directly responsible for designing the plane during the design phase and were delineated into the Wing Team, Propulsion and Mission 2 Team, the Fuselage and Gear Team, and the Tail and Mission 3 Team. A Manufacturing Team, comprised of members from other teams, was responsible for learning and testing new manufacturing methods, and for leading the manufacturing phase when it began. An Integration Team made up of team and project leads made oversight and the integration of various systems possible, and a Business Team was responsible for administrative and finance-related tasks. The structure of the team is shown in Figure 2.2.
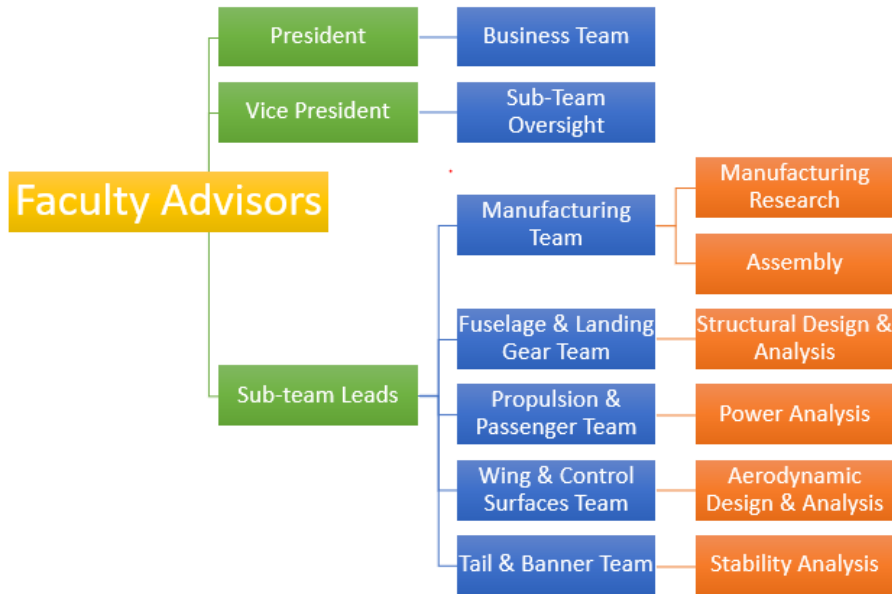
Figure 2.2: Leadership and team structure for Design, Build, Fly at the University of Washington

2.2 Milestone Flowchart

Prior to the first team meeting, the lead team developed a milestone chart, which detailed specific deadlines where certain projects needed to be completed. The timeline for different sections in the conceptual, preliminary, design, manufacturing, and testing phases was developed, and the milestone chart was introduced to all members of the organization in the first meeting. The integration team supervised the milestone chart, and ensured that all sub-teams met deadlines and productivity milestones. The critical deadline chart is given in Figure 2.3, and a schedule flowchart is given in Figure 2.4.

Critical Deadlines	
Proposal Due	**10/31/2019**
Design Complete	11/30/2019
Components Finalized	12/31/2019
Construction Complete	2/15/2020
First Flight	2/18/2020
Design Report Due	**2/21/2020**
All Testing Complete	3/31/2020
Competition Begins	**4/16/2020**

Figure 2.3: Critical deadline chart
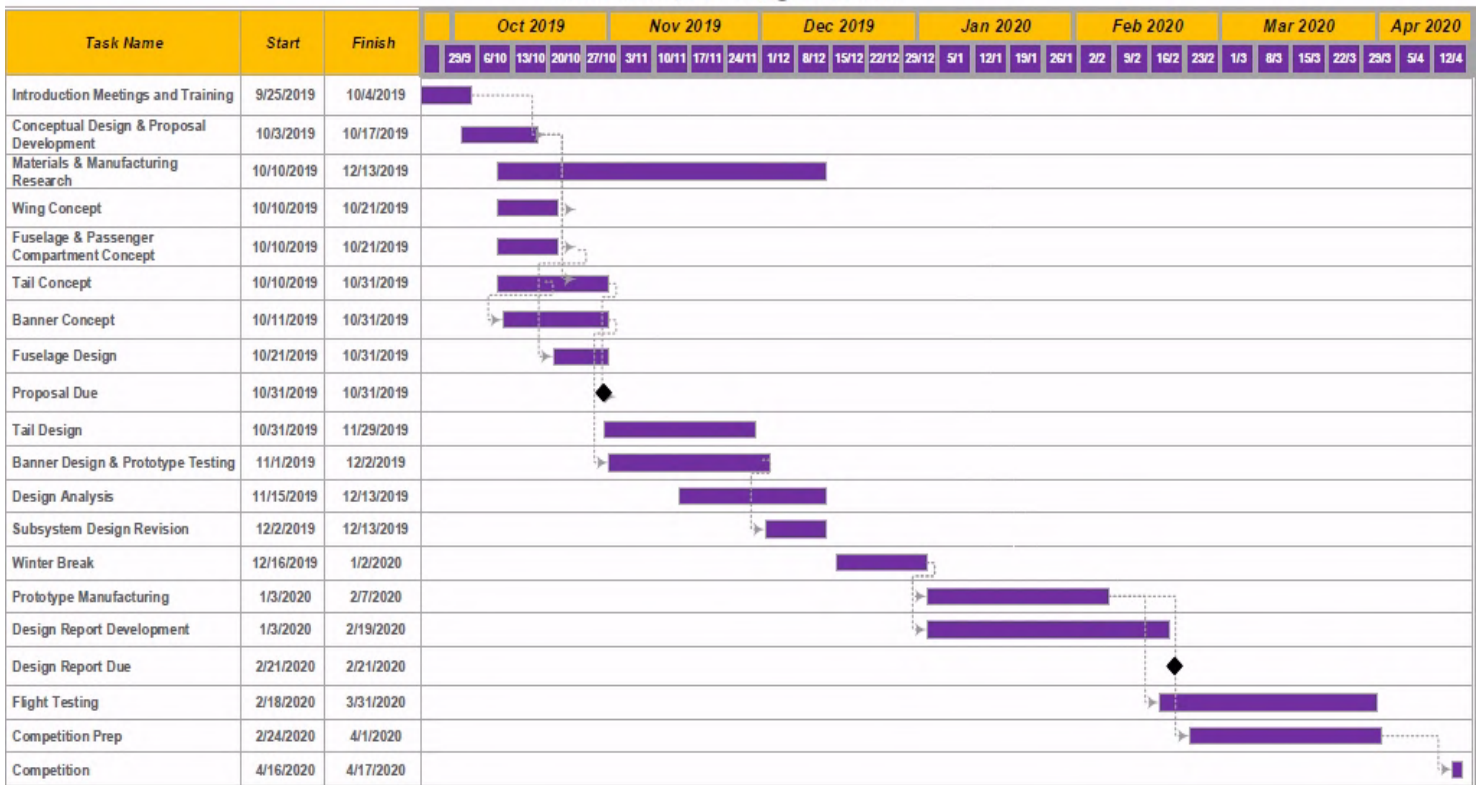
Figure 2.4: Milestone flowchart

3. Conceptual Design

3.1 Mission Requirements and Constraints

|	
■ (red)	Take off
■ (brown)	Climb
■ (yellow)	Cruise
■ (green)	First 180° Turn
■ (light blue)	Cruise
■ (blue)	360° Turn
■ (purple)	Cruise
■ (black)	Second 180° Turn
■ (gray)	Cruise
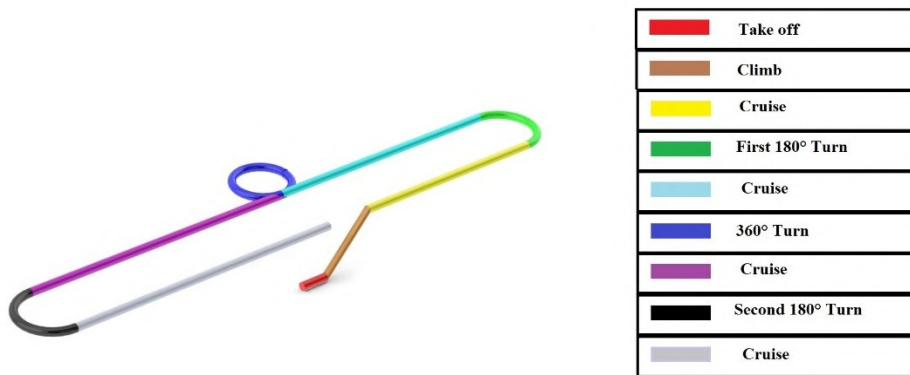
Figure 3.1: Course layout

The total score for the 2020 AIAA DBF Competition is given by Equation 3.1 [1].

$$Total\ Score\ =\ \frac{Written\ Report\ Score \times Total\ Mission\ Score}{RAC}$$ (3.1)

The Written Report Score is scored on a 100-point scale and is based on the quality of the design report. The Total Mission Score is a function of the Ground Score (GS) and the Flight Score (FS). The Total Mission Score is given by Equation 3.2.

$$Total\ Mission\ Score = GS \times FS$$ (3.2)

The Ground Score (GS) is based off of the ground mission and the Flight Score (FS) is the sum of the three individual flight mission scores and is given by Equation 3.3.

$$FS = M1 + M2 + M3$$ (3.3)

3.1.1: Ground Mission

This mission is a timed mission for ground demonstrations of Missions 2 and 3. For the first section, a member of the ground crew must load the passengers and luggage into the passenger mechanism and load it into the aircraft, then the pilot must demonstrate operation of the flight controls. In the second section, the ground crew must remove the passengers and luggage, and successfully mount the banner mechanism with the banner onto the aircraft. For the third section, the release mechanism of the banner must be demonstrated as the aircraft is held vertically, and the banner must be successfully dropped upon pilot command. The time taken for the ground crew member to complete their objectives will be scored as part of the mission score.

3.1.2: Flight Mission 1

The aircraft must take off without any payload on a runway 20 ft in length, and complete three laps within a five minute flight window. The aircraft must then successfully land in order to receive a score as calculated by Equation 3.4.

$$M1\ =\ 1.0\ for\ successful\ mission$$ (3.4)

3.1.3: Flight Mission 2

The aircraft must take off with a passenger and luggage payload. The aircraft must complete three laps within a five minute flight window. Timing ends when the aircraft passes over the start/finish line in the air. The aircraft must then successfully land in order to receive a score as calculated by Equation 3.5.

$$M2 = 1 + [N\_(\#passengers/time)/ Max\_(\#passengers/time)] \qquad (3.5)$$

Where Max_(#passengers/time) is the highest number of passengers divided by time score of all teams.

3.1.4: Flight Mission 3

The aircraft must takeoff with the banner payload within twenty feet. The banner must begin in a stowed configuration, and must be remotely deployed after the first turn. The aircraft must complete as many laps as possible within a ten minute flight window. Once the aircraft has crossed the finish line on the last lap, the banner must be released remotely. The aircraft must then successfully land in order to receive a score as calculated by Equation 3.6

$$M3 = 2 + [N\_(\#laps\ X\ banner\ length)/ Max\_(\#laps\ X\ banner\ length)] \qquad (3.6)$$

Where Max_(#laps X banner length) is the highest number of laps X banner length-score of all teams.

Section 3.1.5: Scoring and Sensitivity Study

$$P = T * v$$

$$q = 0.5 * \rho_0 * v^2$$

$$L = c_L * S * q$$

$$D = c_D * S * q$$

$$Re = \frac{\rho_0 * v * x}{u}$$

$$RPM = V * kV$$

$$D_{ban} = H_{ban} * L_{ban} * q * 0.4046 * (\frac{L_{ban}}{H_{ban}})^{-0.494}$$

$$T = 4.392399 * 10^{-8} * RPM * \frac{d^{3.5}}{\sqrt{p}} * (4.23333 * 10^{-4} * RPM * p - v)$$

$$v_{Prop} = p * \frac{1[in]}{0.0254[m]} * RPM * \frac{0.000423333}{2}$$

$$P_{Actual} = T * v_{Prop}$$

$$solve(\frac{-4.392399 * 10^{-8} * d^{3.5} * RPM * v_{prop} * (v_{m2} - 423333 * 10^{-4} * p * RPM)}{\sqrt{p}} - \frac{c_D * \rho_0 * S * v_{m2}^3}{2} = 0, v_{m2})$$

$$solve(\frac{-4.392399 * 10^{-8} * d^{3.5} * RPM * v_{prop} * (v_{m3} - 423333 * 10^{-4} * p * RPM)}{\sqrt{p}} - \frac{c_D * \rho_0 * S * v_{m3}^3}{2} - \frac{0.2023 * H_{ban} * L_{ban} * \rho_0 * v_{m3}^3}{(\frac{L_{ban}}{H_{ban}})^{0.494}} = 0, v_{m3})$$

$$M_2 = \begin{cases} \frac{\#Passengers}{Time} = \frac{\#Passengers * v}{3 * L_{course}} & Time = \frac{3 * L_{course}}{v} \le 300[s] \\ 0 & otherwise \end{cases}$$

$$n_{p,s} = \lfloor \frac{L_{m2} - W}{W_{passenger} + W_{luggage}} \rfloor$$

$$M_3 = (\#Laps) * (L_{ban}) = \lfloor \frac{v * 600[s]}{L_{course}} \rfloor * L_{ban}$$

$$\hat{M}_{x,i} = \frac{M_{x,i}}{max(M_x)}$$

$$M_{Overall} = \hat{M}_2 + \hat{M}_3$$

Figure 3.2: Equations used in the mathematical model for optimization

The goal of score optimization was to select the configuration that results in the best score before the end of the design phase. This year, the score optimization team implemented a mathematical model based on various aeronautics equations accounting for different parameters. The entire optimization algorithm was developed in Python using Jupyter Lab and was based on robust genetic optimization. The packages used for the scientific calculation were Pandas, Numpy, Scipy, and Matplotlib. Although genetic optimization was slow and often did not output the absolute maximum score, its development was fast and relatively straightforward considering there were several non-continuous functions and step functions in the model. Also, the algorithm was run several times to get multiple advantageous configurations under additional constraints proposed by design teams. The optimization finished before the battery limitation rule change, and optimization does not include Ground Mission and Flight Mission 1, and it was not able to be run after the rules change due to time constraints.

According to the optimization, the relative scores of the best configuration for Mission 2 and Mission 3 are in the 92nd percentile and 95th percentile respectively, which implies that both missions were equally crucial to have obtained the maximum score. Each parameter was weighed against the flight scores. Some examples of these weights are given below.
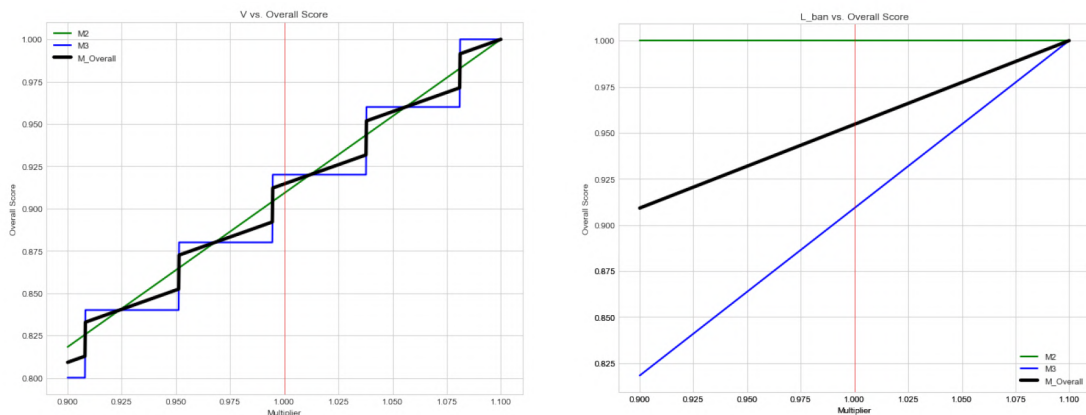

Figure 3.3: Velocity, banner length, and other parameters were weighed against scores

3.2 Configuration Selection

3.2.1 Propulsion System Selection

The main goals of the propulsion system selection were to maximize thrust, minimize weight, and minimize power consumption due to the 200 Watt-hour energy limitation. The required flight time for each mission was estimated, along with a preliminary estimate of the amperage. From this data, several potential batteries were identified, then various motors were examined. From the data of batteries, propellers, and motors, a configuration to provide the highest amount of thrust possible without adding unnecessary tare weight to the aircraft was selected. The 200 Watt-hour energy limitation added a few additional constraints to potential configuration selections. For example, the number of required motors also needed to be minimized, as additional motors would reduce the power supplied to each motor and increase weight. As a result, efficiency and motor weight became high-priority parameters, as the thrust needed to be maximized without exceeding the restriction, and additional system weight would reduce the amount of weight that could be allocated for other aircraft structures and systems.

3.2.2 Empennage Selection

As part of the fuselage and tail design, it was decided that a sloped empennage would be used as a connecting piece between the fuselage and the tail. The goal of the empennage was to maintain the aerodynamic integrity by reducing the pressure drag by keeping flow attached over the fuselage as it transitioned towards the tail.

3.2.3 Avionics Package

The avionics package was originally designed to provide a framework for active stabilization against wind interference, which gave the pilot greater control predictability, and had the ability to collect inflight data. A facet of the controls that was recommended was the implementation of differential thrust, especially once the added drag provided by the banner was considered. This meant that the signals needed to be changed as they came from the receiver, which necessitated an onboard microprocessor. The data collected would include airspeed, positional data, rotational data, voltage, and temperature.

3.2.4 Fuselage Selection

The fuselage, as the central body of the aircraft, must be designed with the integration of all other components kept in mind. Strength, weight, aerodynamics, ease of manufacturing, and several other factors were considered. Certain requirements, including specified mission parameters, were decided upon before any designs were conceived. It was decided that the banner deployment system would not be included within the main fuselage very early on. The passengers and batteries would have to fit inside of the fuselage, which required a large cross section of up to eight inches in width. It was also decided that in order to optimize strength, volume, and weight, the fuselage would consist of a fiberglass shell built around a structure of ribs with four carbon-fiber spars running lengthwise along the fuselage. Four basic cross-sectional designs were proposed: rectangular, rounded rectangular, elliptical, and circular.

Cross-Sectional Layout	Structural Characteristics	Aerodynamic Characteristics	Ease of Manufacturing and Integration
	Corners concentrate stress making potential weaknesses Long flat edges and surfaces can cave in under compression	Potential instability during maneuvers due to rotational asymmetry	Flat surfaces allow for easy integration of wings, empennage, etc. Flat surfaces and orthogonal edges allow for easy manufacture
	Rounded corners distribute stress reducing potential weaknesses Long flat edges and surfaces can cave in under compression	Potential instability during maneuvers due to rotational asymmetry	Flat surfaces allow for easy integration of wings, empennage, etc. Flat surfaces allow for easy manufacture Rounded corners add complexity to manufacture
	Rounded shape distributes stress reducing potential weaknesses Curved edges and surfaces are less likely to cave in	Smooth surfaces and total symmetry allows for greater stability during maneuvers	Curved surfaces make integration of wings and empennage complex Circular shape makes manufacturing difficult

Table 3.1: Characteristics of potential fuselage cross-sections

3.2.5 Landing Gear Selection

The landing gear was designed for mobility and maneuverability on the ground while having minimal negative impact on airborne performance. Both tail-dragger and tricycle configurations were considered during the early stage of design. However, as there was no need for a high angle of incidence, and the tail-dragger configuration had minimal advantages with a short-field takeoff, the tricycle configuration with a steerable nose wheel was selected. Since the nose gear of a tricycle gear configuration absorbs minimal impact during landing, the main gear had to be designed to withstand the bulk of landing impact loads. The nose gear was designed to be steerable, thus a servo needed to be mounted with the landing gear. As the nose gear was not expected to absorb a high load, it was designed with minimal weight.

3.2.6 Passenger Mechanism Design

The passenger mounting mechanism needed to be designed along with the fuselage so that integration could go as smoothly as possible. The ideal passenger mechanism would be able to fit as many passengers as possible into an area so that score can be maximized. Many configurations of passengers and luggage were considered and in the end the passengers would be seated four abreast. This would allow the passenger mechanism to fit within the fuselage.

3.2.7 Banner Design

The scoring calculation showed that a longer banner length optimized scoring, however, the rules indicated that the banner aspect ratio of length/width could be no greater than 5. The rules also stated that the banner must be externally stored and deployed. In addition to these constraints, the banner must maintain a vertical orientation during flight. The banner flutter, or movement, must also be minimal during flight to minimize drag. Another major consideration was banner deployment: the instantaneous drag, or "pull", that the banner exerts temporarily when released caused a major shift in the center of gravity of the plane and exponentially increased drag. Therefore this shift and the addition of drag from the banner needed to be accounted for. When considering material, the banner needed to be permeable enough to minimize flutter but also partially non-permeable such that there is not an overflow of air through the banner. The material needed to be light, such that it could be stowed on the plane with minimal impact to the center of gravity and weight of the aircraft, but not too light or the banner would have been overly sensitive to external changes. The banner deployment and release mechanism needed to be able

to store the banner externally during take off, deploy the banner out of the rear of the plane in a controlled fashion and then drop the banner at the end of the mission. The mechanism also needed to be able to release the banner in a controlled fashion to reduce the rate at which drag increased and the shift in CG when it was deployed.

3.2.8 Empennage Selection

As part of the fuselage and tail design, it was decided that a sloped empennage would be used as a connecting piece between the fuselage and the tail. The goal of the empennage was to maintain the aerodynamic integrity by reducing the pressure drag by keeping flow attached over the fuselage as it transitioned towards the tail.

3.2.9 Tail Selection

Vital to the stability characteristics of the aircraft as a whole and the most probable point of attachment and potentially storage of the banner, the tail design aimed to provide a component sufficiently voluminous to accommodate banner support structures while maintaining reduced drag and control without sacrificing pitch and yaw control authority. These criteria resulted in the favorability of an enlarged vertical stabilizer and remote control surfaces for yaw authority.

3.2.10 Nose Cone Concept

The nose of an airplane was the first component to encounter free stream air, so aerodynamics are the driving factor behind its design and shape. Research showed that a parabolic arc created the least drag relative to other shapes, as shown by Figure 3.4. However, parabolas were difficult to manufacture and model accurately in computerized simulations, so an elliptical nose cone was chosen as it was easier in both regards.

% OF DRAG OF FLAT FACE NOSE
FOR VARIOUS NOSE SHAPES

Comparison of the drag for different nose shapes for a model rocket
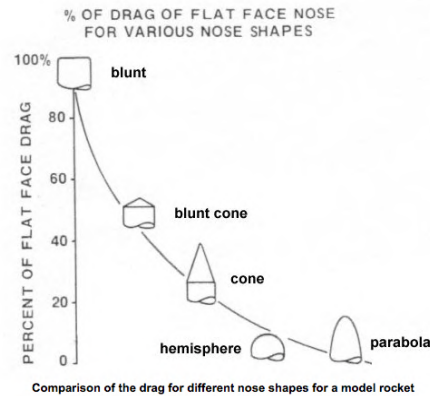
Figure 3.4: Conceptual nose parameters

3.2.11 Airfoil Criteria

Airfoil selection was a crucial part both for ensuring successful takeoff and cruise characteristics of the aircraft. The aircraft must takeoff in a 20 ft distance during Missions 1 and 3, and there was no imposed runway length restriction for Mission 2. Other than these specific requirements, the goal of the airfoil and the corresponding wing was to maximize lift so that the aircraft could carry a heavier load.

4. Preliminary Design

4.1 Design and Analysis Methodology

An iterative procedure was used to design, prototype, and modify the components of the aircraft. For each project, an initial prototype was developed based on the design parameters and requirements determined during the conceptual design process. Integration meetings occurred multiple times a week during the preliminary and detailed design phases to reduce the possibilities of conflicting designs and promote cross-team communication. Due to the complexity of the design, more vital design parameters such as weight, span, and propulsion were developed first.

4.2 Mission Model Methodology

Mission performance was predicted in the preliminary phase through calculations and computational analysis. The approximate time required to complete each mission was first roughly estimated based on experience from the pilot and previous competitions. Each mission was separated into a number of flight stages depending on the requirements of the mission. Several assumptions were also made to simplify calculations.

- The cruise speed at flight was approximated to be a constant 22.3 m/s based on the choices made for airfoils.
- Takeoff was assumed to occur at max throttle within the 20 foot takeoff requirement for the given missions.
- The flight path for each mission was assumed to be optimal, with the pilot making ideal turns and flying straight lines at the straightaways.
- A flight time safety factor of two minutes was added to account for potential deviations.
- Flight conditions were assumed to be seasonally normal for the Wichita area.

4.3 Design and Sizing Trades

4.3.1 Fuselage Design

A circular fuselage cross section was decided upon because of the advantageous structural and aerodynamic characteristics [2]. The fuselage skeleton would be composed of ribs connected by four carbon fiber spars running through the four corners of each rib. In the original design, each rib was required to have space for batteries, the passenger tray, and room for the spars to pass through. To help secure the passenger tray, a guide slot was cut out to prevent

vertical movement of the tray while in flight and allow for smooth sliding. As the design process progressed, the batteries were moved to the front of the fuselage in order to move the center of gravity further forward. The new arrangement left considerable room to remove material and therefore reduce weight. Truss structures were designed to improve the rigidity of the fuselage while also serving as a place to secure the nose gear mount and wires for avionics later in the fabrication process.

| Design Name	CAD Model	Characteristics
Original Design		Accommodates batteries above and below the passenger tray and four square spars.
Final Design		Optimization for weight savings and addition of trusses.
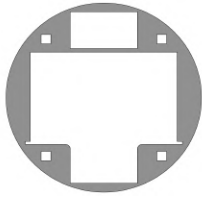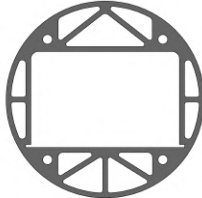
Table 4.1: Ribbing designs
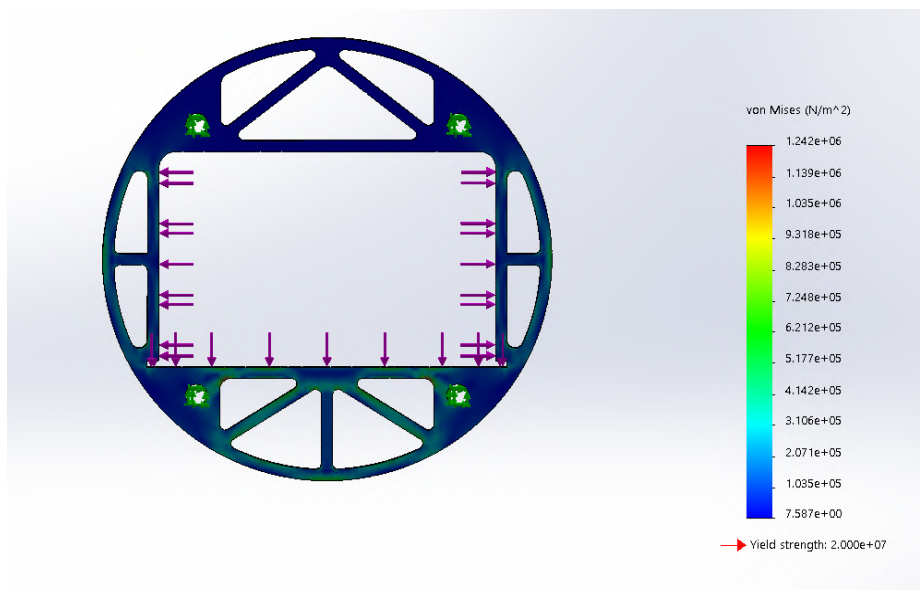
Figure 4.1: Stress analysis on the fuselage ribbing

Basic FEA simulations were carried out on the final model to ensure its structural integrity. A load of 5 lbs on the bottom of the passenger tray compartment and 4 lbs on each side were used to simulate an extreme loading condition during flight. The results, as shown above, were all below the critical yield points, indicating sufficient structural integrity of the final design.

4.3.2 Forward Nose Section

When preliminary analysis was conducted for the nose, the difference in drag between elliptical and parabolic cones was very minimal, making the elliptical nose cone a clear choice for its ease of manufacturing and aerodynamic benefits [3]. The equation for the chosen curve was $y = 8\sqrt{1 - \frac{x^2}{16}}$. Another consideration in designing the nose was accessibility to the passengers and electronics inside the fuselage. Different methods for attaching the cone so it could be removed or swung up or to the side when loading passengers were considered, including external hinges, internal cabinet-like hinges, and a fully-removable nose cone that slides on and off the fuselage spars. The nose cone was locked to the fuselage during the flight through the installation of neodymium magnets. The nose was designed to have a thin shell of fiberglass as its exterior shell, with balsa wood ribs for structural integrity. The nose was iteratively redesigned to fit new components. The final design had four ribs with a 3D-printed tip attached to the front.
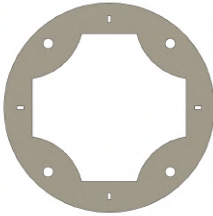
Original Design		Holes for spars to interface and space for servo batteries to fit into the nose.
Final Design		Additional space added for batteries and battery wiring.
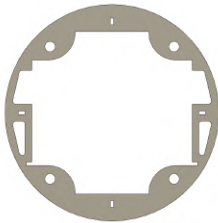
Table 4.2: Forward nose section ribbing

4.3.3 Empennage Sizing
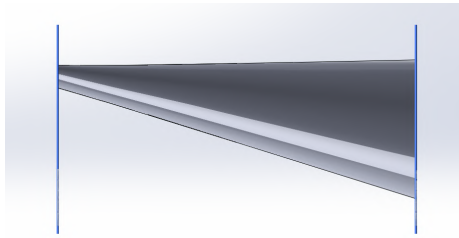

Figure 4.2: Original empennage design   **Figure 4.3:** Final empennage design
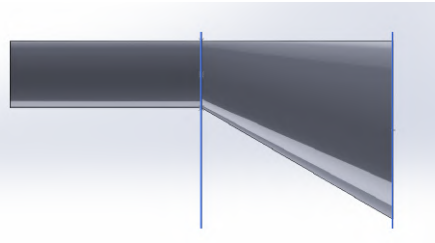
The original design for the empennage was created so that the tail would taper for the entire length of 19 in. Although this was better aerodynamically, the decision was made to taper the tail for 9.5 in due to the significant reduction in weight achieved through a shorter taper. The elliptical shape at the end was also rotated so that it's major axis lies vertically, not horizontally. This was done so that the distance that the carbon fiber spars run through the tail is maximized, which increased stability.

4.3.4 Airfoil Selection

As natural vibrations produced by the semi-rigid landing gear and the subsequent opportunity for structural gear failure that long takeoff distances introduced, takeoff distance was still optimized to be minimal. Airfoils were analyzed at a Reynolds number of 450,000 using XFoil 2-D analysis with Ncrit value of 9. The two airfoils with the best aerodynamics characteristics were chosen and further analyzed, they are shown in Figure 4.4. The NACA 4412 airfoil was chosen over Clark Y for three main reasons. First, to maximize the number of passengers, the wing needed to generate the greatest amount of lift in the range of 0-5 degrees AOA for the given span limitation of 5 ft. From the data in Figure 4.4, the NACA 4412 airfoil accomplishes the goal and surpassed the Clark Y performance. Second, carrying a substantial amount of load on an airplane required a structurally strong and durable wing. Given that the NACA 4412 has greater thickness when compared to the Clark Y with the same chord length, it made the NACA 4412 airfoil a better and more promising choice to decrease the risk of structural failure. Lastly, in order to extend the flight time, minimum power used during cruise, regulated by the ratio $\frac{CL^{3/2}}{CD}$, is required to be at its maximum value. Figure 4.5 represents the relation of previously mentioned

value to the AOA. The NACA 4412 surpassed the Clark Y airfoil and provided lower power requirements for cruise flight. Drag coefficients were studied at corresponding lift coefficients as shown in Figure 4.6. It was found that the drag increase for the NACA 4412 airfoil was extremely low, while the lift coefficient had a substantial increase.
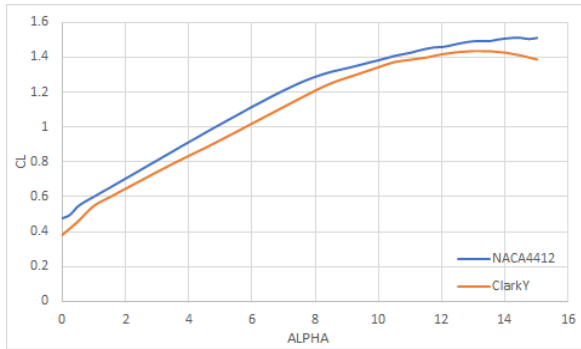

**Figure 4.4:** Lift coefficient vs AOA
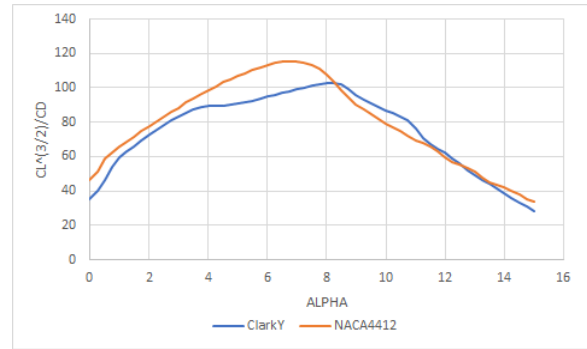
**Figure 4.5:** $\frac{CL^{3/2}}{CD}$ vs AOA
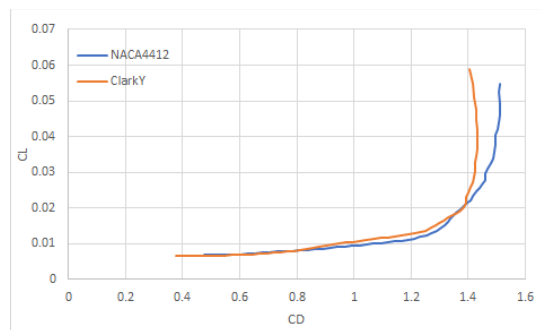
Figure 4.6: Lift coefficient vs Drag coefficient

4.3.5 Banner Sizing and System

Initial banner sizing was calculated at 5 ft x 1 ft given conceptual constraints. Several materials for the banner were considered, including different types of cloth and other materials such as paper, netting, or mesh. Uncoated, silicone and polyurethane-coated, as well as coated diamond weave nylon were identified as the best options. A folding, rigid banner was also explored but discarded. Initial conceptual design of the banner considered a towline, but a mounted mechanism maximized banner stability and helped to ensure that the banner remained vertical. One initial idea had the banner directly connected to the rudder, but since this eliminated rudder authority, it was decided to use two smaller outboard rudders. The banner was rolled in a

rod that was released from the plane along with the banner. Weight optimization was also considered due to the large impact on the center of gravity. As such, solutions proposed for the tail had to keep the number of servos and components to a minimum. Additional ideas proposed included a motor for the spool in the bottom of the empennage or a passive banner deployment system that relied on drag to unroll the banner, but all of the passive systems required a mechanism to unlock the banner and were discarded. It was also determined that there would not have been enough drag on the banner to deploy it, so a controlled deployment system was unnecessary. The rotating slot mechanism was favored due to the forces required to release the banner. To lock the banner in place, a toothed gear with a pin was used. After banner testing revealed that the banner drag was far less than expected and the feasibility of 20 inch tall tail was proven, the mechanism was scaled up with a longer rod and a slightly larger spool, but was otherwise unmodified. A 5-gram servo was selected, based on CAD-modelled stress analysis and torque calculations.

4.3.6 Tail Sizing

In order to maintain a low tail weight while accommodating banner support structure, the initial tail design favored a T-tail. With the potential for reduced drag during mission 3 with the banner both stowed and deployed, a vertical stabilizer of extended height above and below the fuselage was also favored. Tail sizing involved iteratively calculating static margins and stability parameter magnitudes. Based on the characteristics of a NACA 4412 main wing and a NACA 0008 airfoil for the tail, combined with the cg-preference for a 24 inch wing AC to tail AC, the horizontal stabilizer was designed to be 20 inches in span, 7 inches in chord, and 3 degrees in tail setting angle. The NACA 0008 was chosen for its symmetrically simple manufacturability and its low weight per unit span.

This arrangement further held the theoretical potential for reduced drag and reduced horizontal stabilizer size due to reduced downwash from flow over the wing. The possibility of instability and increased structural complexity however spurred an investigation into the flow characteristics over a conventional tail, a cruciform tail, and T-tail. Analyzing each configuration with a basic fuselage and vertical stabilizer, and the preliminary wing design, it was determined that with the horizontal stabilizer's AC positioned approximately 24 inches behind the wing, it was determined that for low angles of attack, at which a general stall would be unlikely, there is minimal to no downwash flow influencing flow over the tail, reducing the need for a T-tail. Thus a

conventional tail was chosen in the end. To reduce drag and provide sufficient structural integrity, the vertical stabilizer was dedicated to the banner mechanism. With a banner stowed in the tail for mission 3, no room was left in the vertical stabilizer for a rudder, necessitating the design of rudders placed at the tips of the horizontal stabilizer. With a location akin to those of winglets on a main wing, these rudders have the additional benefit of increasing the efficiency of the horizontal stabilizer. Tail ribbing for banner support was iteratively designed through Fusion360 FEA analysis and revision to produce desired load paths.
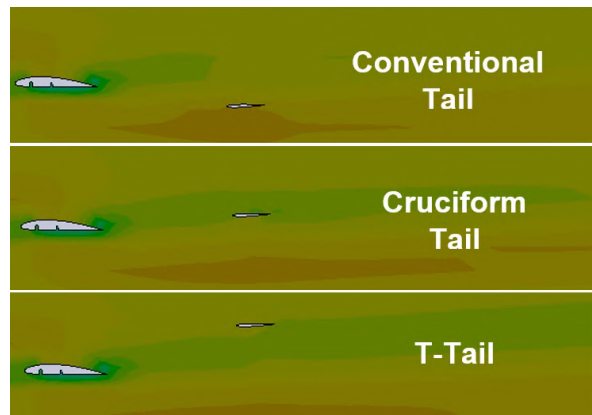

Figure 4.7: Arduino chip comparison

4.3.7 Controls optimization

Based on the necessity for manually processing signals from the receiver, it was clear that a microprocessor was necessary. Arduino boards were the most widely used, and analysis was performed on which to select based on size, weight,minimum speed, and memory [4]. It would have been possible to implement all the controls without using an Arduino, but this would have been far more difficult, especially concerning the banner release mechanism. Efficiency testing revealed the best way to gather input from the receiver was to use a function of Arduino called an interrupt as opposed to Arduino's PulseIn method. While PulseIn had to pause and wait for a signal, an interrupt allowed the chip to multitask, which increased efficiency by a factor of roughly 30,000, which subsequently greatly reduced the latency of controls. The ATmega328 performed at roughly 20 MHz according to specifications, which gave 20,000 operations per microsecond. Since a call to PulseIn consumed 1.5 microseconds of power, the Arduino could have performed roughly another 30,000 (20,000 * 1.5) operations during that time. An interrupt-driven approach allowed the chip to perform operations between readings, which greatly

reduced latency in the controls. There were three initial chips that were considered, but there are some accessibility features of the Uno that made it easier to use and connect to I2C devices, such as a gyroscope.

Chip design	Arduino Nano	Arduino Uno	Arduino Mega
Weight	3	1	0
Size	3	2	1
Memory	1	1	2
Input/Output Capacity	2	3	4
Value	10	7	7

Table 4.3: Arduino chip comparison

4.3.8 Propulsion System

It was first determined that lithium-polymer batteries would be the optimal choice for powering the propulsion system as they provided the most power while maintaining a relatively low weight. In addition, it was decided that any motors would not be mounted on the nose, so that the nose was able to be used to quickly gain access to the passenger compartment. The aerodynamic impact of motors on the wings was also considered, and it was decided that some type of cowling would be used to reduce the profile drag of the motors. Based on the parameters and possibilities discovered during the conceptual phase, specific potential components of the propulsion system were analyzed. It was estimated that the aircraft would require a flight time of at least 10 minutes, which, considering the 200 Watt-hour limitation, meant that two five or six cell LiPo batteries would balance the necessary output and operating time that was necessary to fly all the missions. A list of potential batteries was drawn up from local and online sources and matched against the dimensions of the battery-mounting mechanism that could be placed within the limited confines of the aircraft, and it was decided that Turnigy batteries were to be used due to their low cost. Considering the harsh restrictions on power, as well as the need to easily access passengers, it was determined that two motors would provide optimal results. Afterwards, the main limitation to the motors that could be used was cost, as the budget allocated for propulsion

was heavily constrained. Both a TGY Propdrive v2 5050 580KV Brushless Outrunner Motor and a Scorpion SII-4020-630KV Motor were considered. The TGY motor was much less expensive, and would've allowed for a large number of motors to be purchased for testing. However, the Scorpion SII was much lighter and more efficient, so the aircraft was equipped with those specific motors.

The sizing of the propeller was also narrowed down based on conceptual decisions [5]. Once battery and motor were decided, the goal became to find the propeller that would provide the highest level of thrust that could be adequately utilized with the current configuration. It was also decided that carbon fiber would be the propeller material due to its relatively low cost and high durability compared to plastic or other options. A 15x4W propeller was ultimately mounted on the engines as part of the final propulsion system.

4.3.9 Wing Geometry

In order to approximate the wing area needed to take off for both Missions 1 and 2 with the given set parameters, such as thrust of 26 lbf and aircraft weight approximated to be 13 lbs for the unloaded configuration, a constraint diagram was plotted in MATLAB for both takeoff and cruising flight conditions. A constraint diagram, which plots thrust to weight ratio against weight to wing area ratio is shown in Figure 4.8. To maximize the number of passengers given the fixed wing cross section and 5 ft span limit, chord length was maximized to generate the greatest amount of lift. For better performance, the aspect ratio could be no less than 4. Preliminary lift calculations were performed for various wing areas, which fell between 5 and 5.75 ft^2. Using the constraint diagram and wing areas mentioned previously, the maximum takeoff weight of an airplane for M2 was estimated to be 18.3 lbs, accounting for a factor of safety of 1.2 with a takeoff distance of 60 ft. Given the thrust values and weight estimate, wing area was estimated to be 5.25 ft^2, which corresponded to a chord length of 1.05 ft and an aspect ratio of 4.76.
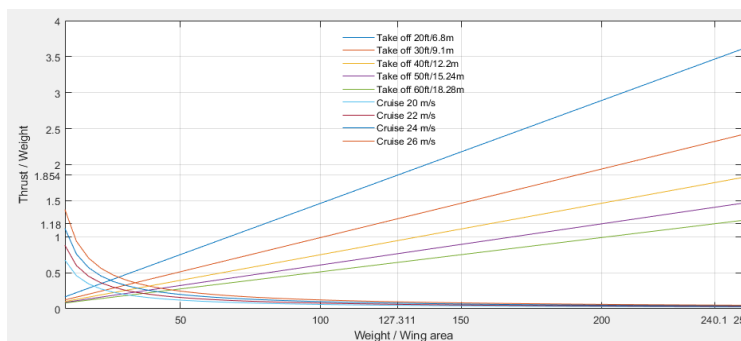

Figure 4.8: Constraint diagram

4.3.10 Passenger Mechanism

Passenger Configurations (30 Passengers)	Width Min.	Length Min.	Decisions
3 Rows	3.75"	12.5"	Too long and narrow
4 Rows	5"	10"	Good length and width
5 Rows	6.25"	7.5"	Too large of diameter

Table 4.4: Passenger tray sizing

The luggage was put in front of the passengers in order to bring the center of mass of the tray, and therefore the plane, as forward as possible. Of the types of designs considered, the two level sliding tray was chosen because of its superior structural integrity, lightness, and its ease of manufacture. The tray was inserted through the front of the plane and the nose followed, which locked the tray in place. The floor was lined with a thin layer foam in order for the passengers to be secured and not contact one another. In order to make access easier and prevent vertical motion, it was decided to have the floor extend to the edges which formed rails within the fuselage. The luggage was held in the tray by a door that slid in and out vertically.

It was decided early on that a rectangular design would be used due to its ease of manufacture, as well as the ability to easily fit it into the existing fuselage design. It was also quickly determined that a sliding mechanism, accessed from the nose, was optimal for the ground mission. The loading speed was further optimized by having the ground crew member be allowed to quickly drop the passengers into the tray. The main goals of the passenger tray were to save weight and to maximize the amount of passengers in the space allowed. From the first design, prototypes were manufactured and analyzed. In order to be flexible with the situation so that there was a tray that works perfectly with the fuselage, three sizes of tray were designed for 16, 20, and 24 passengers.

Prototype	Images	Benefits	Potential Issues
1		Able to fit passengers well	Needs to be lighter, Can't hold enough luggage
2		Can fit proper luggage amount and is lightweight	Modular and adaptable to different sizes

Table 4.5: Multiple versions of the passenger tray

There were several methods that were considered for restraining passengers. Preliminary ideas including a wire-like cage, a thin foam sheet, or a rigid wood sheet. All of these options were relatively inexpensive and light, so all of these options were heavily explored before a final decision was made.

4.3.11 Landing Gear Selection

The options considered for landing gear materials and designs are outlined in the table below.

Name	Image	Characteristics
One-piece landing gear (selected for ease of construction)		Simple design Easy to construct and maintain,
Linear struts		Excellent impact absorption Durable
Frame with tension spring		Lightweight and durable Excellent impact absorption

Table 4.6: Main landing gear design options

As the nose landing gear needed to be steerable for ground handling, it needed to withstand high lateral and vertical loads. Steel wire was selected early on due to availability. 3D-printed mounts that relied on a shear joint and were braced against the bottom of ribs were considered. The mount selected was braced between the first and second form ribs, attached to both with matching cutouts.

4.4 Lift, Drag and Stability Characteristics

Lift and drag characteristics were analyzed during the airfoil selection phase, but as those were done under the assumption of infinite wings, some additional work needed to be completed for the finite wing. To reduce wingtip vortices, consequently increasing lift and reducing drag, winglets were added to the aircraft. The iterative process began by making a CAD model of the wing in Solidworks and running CFD simulations on it to determine lift and drag values [6]. After that, taking a lead from the Aviation Partners winglets fitted to the Boeing 737, an altered version was designed. After running a CFD analysis, it was found that due to the thick chord length of the straight wing, the blended winglets added excessive drag. The next design considered was inspired by wingtip fence geometry used by Airbus. It was discovered that while the geometry increases performance, the manufacturing difficulty was high. The design was then moved toward a winglet design that tapered back, with a pointed flat plate. A very thin (approx. 1/16th inches) pointed flat plate was selected for the competition aircraft shown in Figure 4.9. This flat plate achieved the goal of having an increase in lift by 27% while reducing the drag by 15.4%. This design also minimized the increase of the aircraft's empty weight. Since the winglets extended several inches above and below the wing, they were designed to be strong, yet shear off the wings to minimize impact to the wing, if the airplane was to tip-strike. To this end, winglets were manufactured such that the interior of the winglets was made of a 1/32nd inch sheet of balsa wood due to its light weight and foundational capability. The exterior of the winglets were made with carbon fiber to increase structural rigidity and stability.
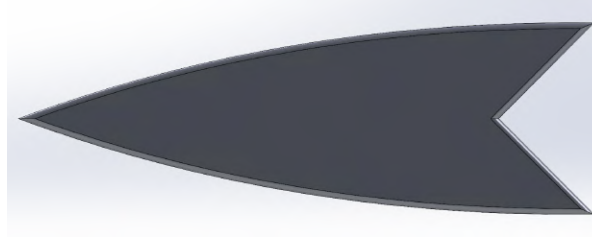
Figure 4.9: Winglet design

4.5 Predicted Aircraft Mission Performance

Taking the preliminary designs of the nose, wing, fuselage, empennage, landing gear, and tail, the progress of the design was tested through CFD simulation in SolidWorks for possible wing *i* of 0 and 4 degrees, AOA of 0 and 5 degrees, and airspeeds of 18, 20, and 22 m/s. These simulations confirmed the benefit of manufacturing with the wing at an *i* maximizing Cl/Cd. Despite increasing manufacturing complexity, increasing *i* to 4 degrees provides an average of 77% more lift with negligible increase in drag. Computational results also verified propulsion calculations by providing numerical drag values for checking required power during cruising flight.


Predicted Aircraft Parameters

	18 m/s 0 deg AOA	20 m/s 0 deg AOA	22 m/s 0 deg AOA	18 m/s 5 deg AOA	20 m/s 5 deg AOA	22 m/s 5 deg AOA
Lift [N], i = 0 deg	15.08	19.40	23.73	46.12	56.93	69.56
Lift [N], i = 4 deg	31.28	38.49	46.55	70.43	87.86	106.66
Drag [N], i = 0 deg	7.1839	8.8683	10.6952	5.7305	7.0273	8.3829
Drag [N], i = 4 deg	7.8000	9.6566	11.6459	5.1224	6.2280	7.4423
Pitching Moment [Nm], i = 0 deg	-1.33	-1.74	-2.19	-9.74	-11.99	-14.62
Pitching Moment [Nm], i = 4 deg	-3.51	-4.23	-5.14	-13.78	-17.13	-20.74

Figure 4.10: Performance parameters for missions 1 through 3

5. Detail Design

5.1 Dimensional Parameters

Fuselage		Vertical Tail	
Total Length (Tip to Tail)	47.5 [in]	Profile Span (height)	19.6 [in]
Nose length	8.0 [in]	Base Chord	6.0 [in]
Empennage Length	19.0 [in]	Tip Chord	3.4 [in]
Tail length	7.0 [in]	Maximum Thickness	2.0 [in]
Fuselage Width	8.0 [in]	Rudder Height	5.2 [in]
Fuselage Height	8.0 [in]	Rudder Base Chord	6.0 [in]
Profile Height	28.3 [in]	Rudder Tip Chord	3.0 [in]
Wing		**Horizontal Tail**	
Airfoil	NACA 4412	Airfoil	NACA 0008
Span	59.5 [in]	Span	21.0 [in]
Chord (non-variable)	12.6 [in]	Chord	7.0 [in]
Wing area	1499.4 [in^2]	Maximum Thickness	0.6 [in]
Aspect Ratio	4.72	Wing Area	294 [in^2]
Angle of Incidence (deg)	4	Aspect Ratio	3
		Angle of Attack (deg)	-1.5

Table 5.1: Aircraft dimensions

5.2 Structure Characteristics and Capabilities

5.2.1 Motor Pylon

The motor mounts were designed to fit the Scorpion SII-4020-630KV motor, a commercial motor with 48.9 mm diameter and 48.45 mm length. In order to mount the motor, it was mounted behind the mounting surface in order to accommodate the cowling. Each motor was directly mounted onto the interior face of the mount with four screws. Wires were run inside the mount along the wing spars to the fuselage, where they connected to the control and power systems. The motor mounting surface was also canted by four degrees to provide more effective lift on the plane. It was also decided that the motor mount would be designed with convenience in mind, namely in ease of manufacturing, weight, and integration with the wing system. The motor mount was designed such that it fits over the wing spars and the upper surface was flush with the upper surface of the wing, reducing any impact the mounting system had on aerodynamics. FEA was also used to ensure that the motor mount did not incur a structural failure during flight.

5.2.2 Wing Spar Structure

Carbon fiber tubes were used to connect wing sections to prevent bending. They also directly mounted to the wing brackets which allowed for mounting into the main wing support in the fuselage. The tubes also had a higher Young's Modulus of Elasticity than the foam and laminar composites that increased the overall stiffness of the wing and reduced bending due to aerodynamic loads during flight.

5.2.3 Landing Gear Structure

The nose gear was designed to be steerable, so it had to be free to rotate. A design was chosen with the servo mounted vertically right behind the landing gear to keep the servo arms and the linkage inside the fuselage, which made the module compact.
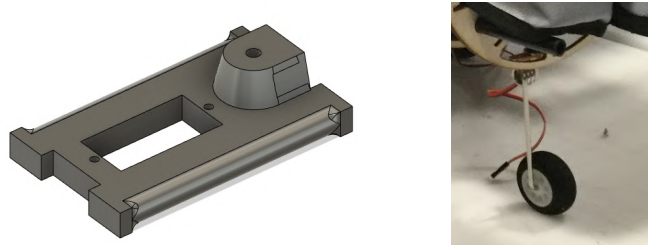

Figure 5.1: Steerable nose gear

A single, continuous aluminum piece was used for the main gear due to its ease of construction, durability, and low drag profile. The plate was mounted to the carbon fiber fuselage structure using a laser-cut birch wood box designed to fit around the bottom longitudinal rods between fuselage form ribs. The main gear was mounted near to, but behind the center of gravity location to minimize the force needed to raise the aircraft's nose on takeoff.
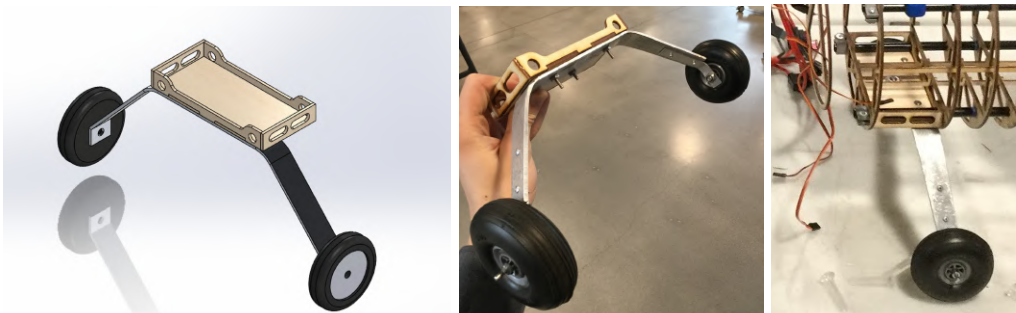
Figure 5.2: Main landing gear mount

Once the structural complexity and lighter takeoff weight were considered, a hardened single piece aluminum landing gear mounted to the fuselage was selected as the focus of design.

5.2.4 Passenger Tray Structure

It was decided to have the passenger tray hold the propulsion batteries due to the size of the batteries. In order to accommodate this change, the door design was modified and parts were attached such that the batteries were successfully held in place with the required distance between them. The final tray was designed to hold a maximum of 24 passengers, and a luggage compartment was placed in front of the passengers. The passengers were added or removed from the top, and each passenger was secured by a top and bottom section that prevented motion along the x-y plane. In addition, the holes were tight enough that it was difficult for the passengers to move vertically, so the design proved to be adequate for passenger load security.

The luggage compartment was accessed from a sliding door. The luggage compartment itself had a floor, roof, and sides that held the luggage secure in place, and the door slid up to allow for luggage to be added or removed. The sliding door was also used to support the batteries, which held them at the required 0.25 in apart. One battery was mounted against the floor and held down with two brackets, while the second battery was held by four brackets, such that it was suspended above the other battery.

5.2.5 Fuselage Details

As the fuselage is at the center of the aircraft, integration with the other components of the aircraft was a key consideration during its design. Due to the number of components that the fuselage had to be built around, it was decided that an irregular rib spacing was needed, with ribs spaced at 2-3 in intervals, as determined by prior prototype testing. To start with, there were a few positions where a rib was required. These positions were at the very front and rear ends of the 12.5 in long fuselage, and at the ends of each passenger tray configuration, in order to provide support for the passenger tray. Based on these requirements, ribs 1,5,6, and 7 were positioned at 0", 8.270", 9.645", and 12.5" from the front of the fuselage respectively. Additionally, ribs did not go between 6.142"-6.886" and 10.659"-11.403" due to interference with the wing mount.
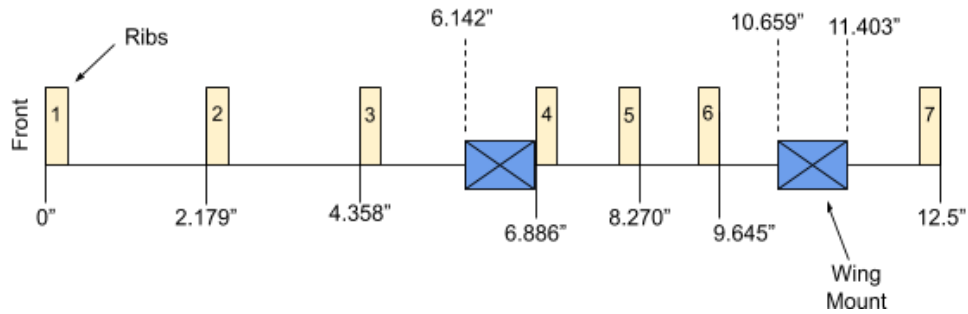
Figure 5.3: Side-view diagram for the fuselage ribbing

Rib 3 was positioned directly in front of the leading edge of the wing, in order to provide full support for the fiberglass skin. The remaining ribs, 2 and 4, were positioned so that the spacing between consecutive ribs was as close to the optimal spacing of 2-3 inches. In order to integrate the fuselage with the rest of the plane, many of the ribs had to be modified based on their specific positioning in the fuselage. The following chart shows the modifications that had to be made to individual ribs in order for them to fit with the other components of the aircraft.

Ribbing number #	Design Model	Description
1-2		The bottom part of ribs 1 and 2 had to be modified in order for the nose landing gear to mount to the fuselage.
4-6		The top section of ribs 4, 5, and 6 had to be removed in order to fit around the wing mount/wing.
7		The top section of rib 7 had to be flattened so that it didn't interfere with the wing. Additionally, space had to be made in the rib to allow the tail spars to pass through to the wing mount.

Table 5.2: Rib structure

In order to increase structural rigidity of the fuselage, stringers were designed with notches to hold the ribs together, which ran through the holes in the ribs. The stringers were also made of 3 mm thick wood, like the ribs themselves. Four stringers were positioned in the sides and bottom of the fuselage.

**Figure 5.4:** Spacers to hold ribs in place

5.2.6 Nose Construction
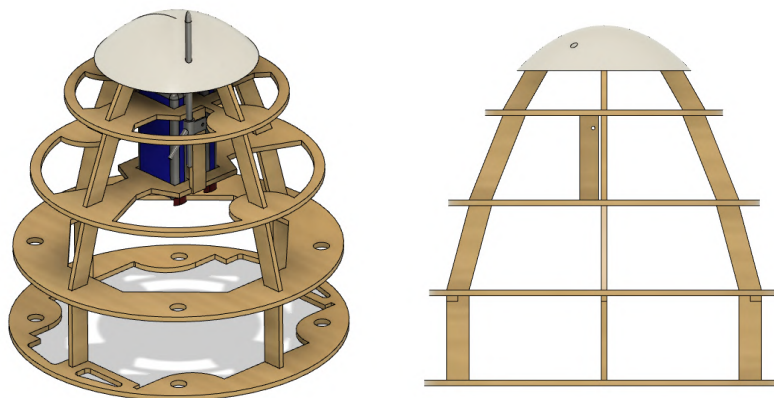
Figure 5.5: Nose cone structure

The nose cone ribbing was developed to conform to the shape of the fiberglass nose cone that was laid over it and fit over the 4 carbon fiber spars that run the length of the plane. Each rib had notches cut out where the 4 wood posts of each layer held all the ribs in the correct position. The top rib/cap is designed to hold the pitot tube out in front of the nose with the 2 ribs below designed to accommodate 2 avionics batteries. The 2 bottom ribs had a large gap in their center section for containment of the forward main battery. Cuts were made on the edge of the bottom rib to allow for wires from the avionics battery to pass into the fuselage. There were 2

notches on the inner edge of the bottom rib that were also made to fit the passenger tray. Lastly, all but the top rib were optimized for weight and material saving. The top rib was optimized for structural support as this held the brunt of the wing stress, and this was also a critical area for fuselage support.

5.2.7 Tail and Empennage

The internal structure of the empennage was composed of two carbon fiber spars spaced apart to reduce torsion on the tail while incorporating a taper for aerodynamics and weight reduction. Attached to the spars were 1/8th in thick balsa wood ribs that served to keep the two spars at a fixed distance from each other. They also served to maintain contact with the skin. One of the ribs was modified to mount the avionics package, and all of the ribs had material removed to optimize structural weight, which also allowed for wires to pass easily through. Added stability is provided by a fiberglass skin which will provide surface tension, and by a cord connected directly from the main fuselage to the tail.

The tail of the plane consisted of a foam core with fiberglass balsa composite horizontal stabilizer, and a wood frame with covering film for both the vertical stabilizer and the rudders. All wooden frame components possessed holes and other lightening features and were made out of 1/8th in thick plywood. With some 1/16th in balsa wood supports, these components were streamlined with covering film to provide an airfoil. On the edges of the horizontal stabilizer are 2 rudders that were articulated by 2 5 gram servos, which were attached to edges of the horizontal stabilizer. The rudders were secured in place with a 3D-printed connector. The horizontal stabilizer was a NACA 0008 airfoil that had a carbon fiber spar which ran through the middle of it to provide support. The stabilizer was then covered in a layer of balsa wood and fiberglass.

5.3 Subsystem Design

5.3.1 Propulsion System

The motor mount was manufactured with 2 spaced slots such that each one was directly mounted into the wing spars while remaining flush with the upper surface of the wing, minimizing airflow disruption. The motor was mounted inside the mount, and the aerodynamic cowling was mounted under the motor such that air was pulled inward to cool the motors. Wiring for each motor was run alongside the wing spars into the fuselage, where it was then connected to the Arduino unit and propulsion batteries. The total amount of thrust produced by these motors was

calculated to be around 18 lbs. This figure included efficiency factors. The resulting flight time, calculated from the capacity of the power supply and amperage draw, was 12 minutes, which would allow the aircraft to successfully complete each mission with a small factor of safety without running out of power.

5.3.2 Servo Selection

Selection of the servos utilized for actuation of banner release, nose gear, and control surfaces was based upon 4 criteria: servo torque, reliability, size, and cost. For the actuation of large, mission critical control surfaces such as flaps and ailerons, servo torque and reliability were prioritized, resulting in the selection of metal-geared TGY servos. Except for the rudder-actuating servos, other servo applications utilized low-cost generic 9-gram HXT servos. The rudder servos were dimensionally constrained, so thin TGY Twin BB servos were selected for their thinness despite increased cost. Please see section 5.6 for specific sevo models.

5.3.3 Control Systems

This design had no noticeable latency and recorded data from all necessary sources to an SD card without any trouble or lack of speed. It also helped the pilot by implementing differential thrust, which helped the plane turn easily, despite the large vertical stabilizer. The avionics package was restricted to three main tasks: gathering data from the pitot tube and gyroscope/accelerometer, deploying the banner smoothly, and optimizing pilot control of the airplane. Aileron, rudder, elevator, and throttle controls were routed through the Arduino. Differential thrust was implemented during flight by changing the throttle input according to the rudder's displacement from neutral. The positioning of the banner servo was not consistent with the controls, so the banner input was modified and passed on to ensure proper banner positioning. Finally, the raw data gathered from the gyroscope and pitot tube were interpreted and written to an SD card module for later processing. The Arduino measured the time in between signals from the receiver in microseconds, converted microseconds to degrees, and transmitted that information to the appropriate servos or ESCs.
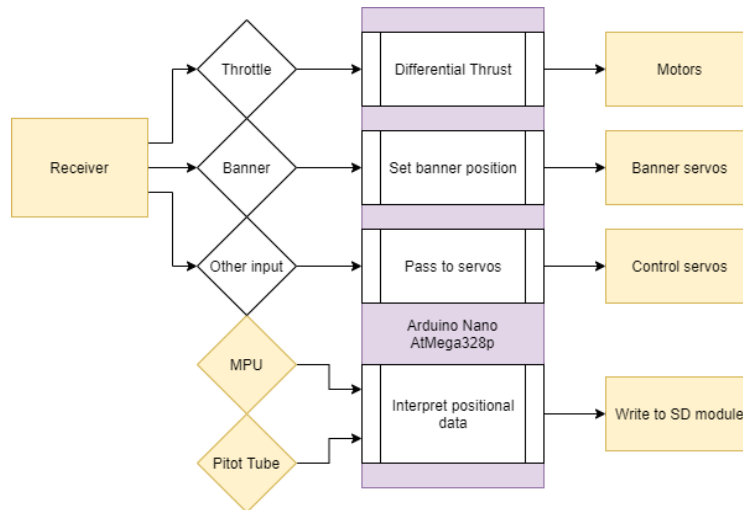
Figure 5.6: Control diagram

The memory and processing speed of the ATmega328P was sufficient for purposes of the avionics package, and final research of the necessary number of pins showed that the Nano was capable. The Nano also had enough capacity for connections to meet the minimum requirements for communication with the various parts of the plane, so it was selected. The design of the differential thrust algorithm was done by finding a percent to change the throttle by, in a way that would account for negative percentages if necessary. To find this percentage, the displacement of the rudder from neutral was measured, a number roughly between -500 and 500 (in microseconds). This number was then divided by a composite called a "transformer," found by dividing the maximum displacement (500) by the maximum percent change that the throttle underwent. The displacement divided by the transformer yields a percentage, which was then added to the left rudder input and subtracted from the right rudder input, due to the direction of the rudder under various inputs.

5.3.4 Banner Design and Sizing

Due to uncertainties of the conditions at competition, it was deemed necessary to have both a 12 in and an 18 in tall banner. The impregnated silicone/polyurethane ripstop nylon material was chosen as it had the lowest overall drag and least damage done to it following the banner tests. The banners were then sewn with 0.75 in hems on the top and bottom edges of the banner, and a 1.5 in hem on the trailing edge, to strengthen and reinforce the edges of the banner

and allow room to sow. The leading edge, however, had a fold over of about 1.5 inches to accommodate the 0.5 in rod that would be used as a spool to roll the banner up for storage and subsequent deployment.
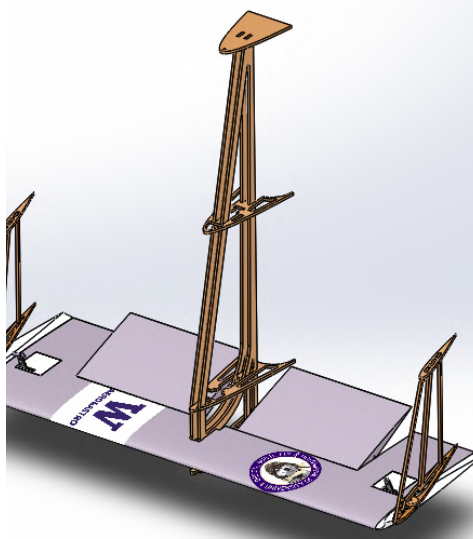

Figure 5.7: Tail interior structure CAD drawing

5.3.5 Banner Deployment and Release Mechanism

      The banner deployment and release mechanism had the banner sliding along a 0.5 in wooden dowel that formed the core of a spool that had 1.5 in diameter rims. The secondary spool below the banner was for an elastic release mechanism to release the banner enough for the drag to release it the rest of the way. To prevent the banner from deploying during take off, there was a lock mechanism that consisted of a toothed gear and a similarly sized tooth that prevented rotation. To both deploy the banner and release it, a locking mechanism that consisted of a circular slot, with a section removed to allow the banner to be pulled out with both drag and gravity. The lock rotated 10 degrees for the banner to move and unfurl and it then rotated another 30 degrees when the banner is released. The lock mechanism was controlled by a 5 gram servo with a linkage arm that connected to the locking mechanism.
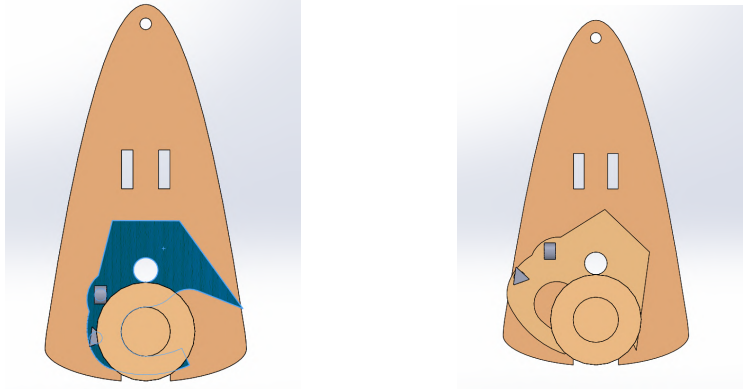
Figure 5.8: Banner locking mechanism

5.4 Weight and Balance

5.4.1 CG Determination

Proper center of gravity alignment is crucial for aircraft stability during flight. The *Phoenix* was designed so that the center of gravity fell within the 3 in region between the leading edge and the aerodynamic center of the wing. This means that without considering other stability aspects of the plane, (notably the tail) the aircraft will have a pitch-down tendency, which was preferred by the pilot. The aerodynamic center of the plane fell at 15.5 in while the CG envelope fell within 14.4 in to 15.1 in with respect to the nose tip as the 0.0 in location. For a 24 passenger Mission 2, the CG does not shift from Mission 1, thus the passenger tray CG is centered at the location of the aircraft CG.
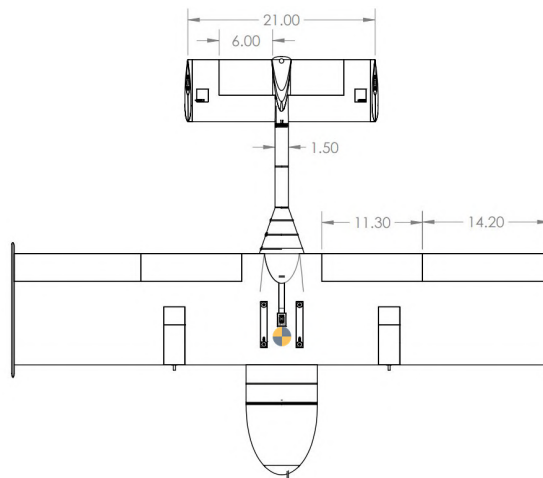

Figure 5.9: Location of the center of gravity envelope

Aircraft Component	Weight [oz]	X [in]	Weight*X [lb*in]
M1 (Empty Flight)			
Auxilary Batteries	4.2	3.0	12.6
Nose (structurals and front gear)	8.5	5.0	42.5
Propulsion Batteries	50.1	7.0	350.7
Motors, Props, Esc's	38.5	13.5	519.75
Fuselage Structurals	10.25	14.3	146.0625
Unloaded Passenger Tray	5.5	14.5	79.75
Wing (not including esc, motor, prop)	55.5	16.5	915.75
Wing Mount	5.25	18.0	94.5
Main Landing Gear	8.5	20.5	174.25
Empennage	6.5	30.0	195
Tail (no banner)	9.5	41.0	389.5
Totals	202.3	**CG Location**	2920.3625
		14.4	
M2 (Passenger Flight: Adding passenger weight to tray)			
Loaded Passenger Tray	144	14.5	2088
Totals	346.3	**CG Location**	5008.3625
		14.5	
M3 (Banner Flight: Adding banner weight to tail stowed)			
Banner stowed	3	41.0	123
Totals	205.3	**CG Location**	3043.3625
		14.8	
M3 (Banner Flight: Adding banner weight to tail unfurled)			
Banner unfurled	3	83.0	249
Totals	205.3	**CG Location**	3169.3625
		15.4	

Table 5.3: Airplane weight and balance

5.5 Performance Parameters

Performance Parameters	M1	M2	M3
Max Cl	1.5135	1.5135	1.5135
Cl average (level flight)	0.534	0.7	0.534
Cd estimation (level flight)	0.04	0.04	0.1867
L/D at cruise	4	4	1.37
Wing Loading	1.213 lb/ft^2	2.077 lb/ft^2	1.230 lb/ft^2
cruise velocity	72 ft/s	72 ft/s	55.2 ft/s
stall velocity	38.13 ft/s	48 ft/s	38.13 ft/s
Aircraft weight	12.64 lb	21.64 lb	12.81 lb
Carried Payload	0 lb	9 lb	0.1875 lb
Number of laps	3	3	12
Misson score	1	1.7	2.5

Table 5.4: Performance parameters for final design

5.6 Drawing Packages

SCALE: 1:20

21.00
6.00
1.50
11.30
14.20
18.00
89.72
136.79

2.16
60.60
.67
1.86
8.47
Ø8.00
13.62

47.29
3.50
12.69
9.47
9.50
12.59
4.00
19.56
8.00
28.25
5.12
8.43
18.34
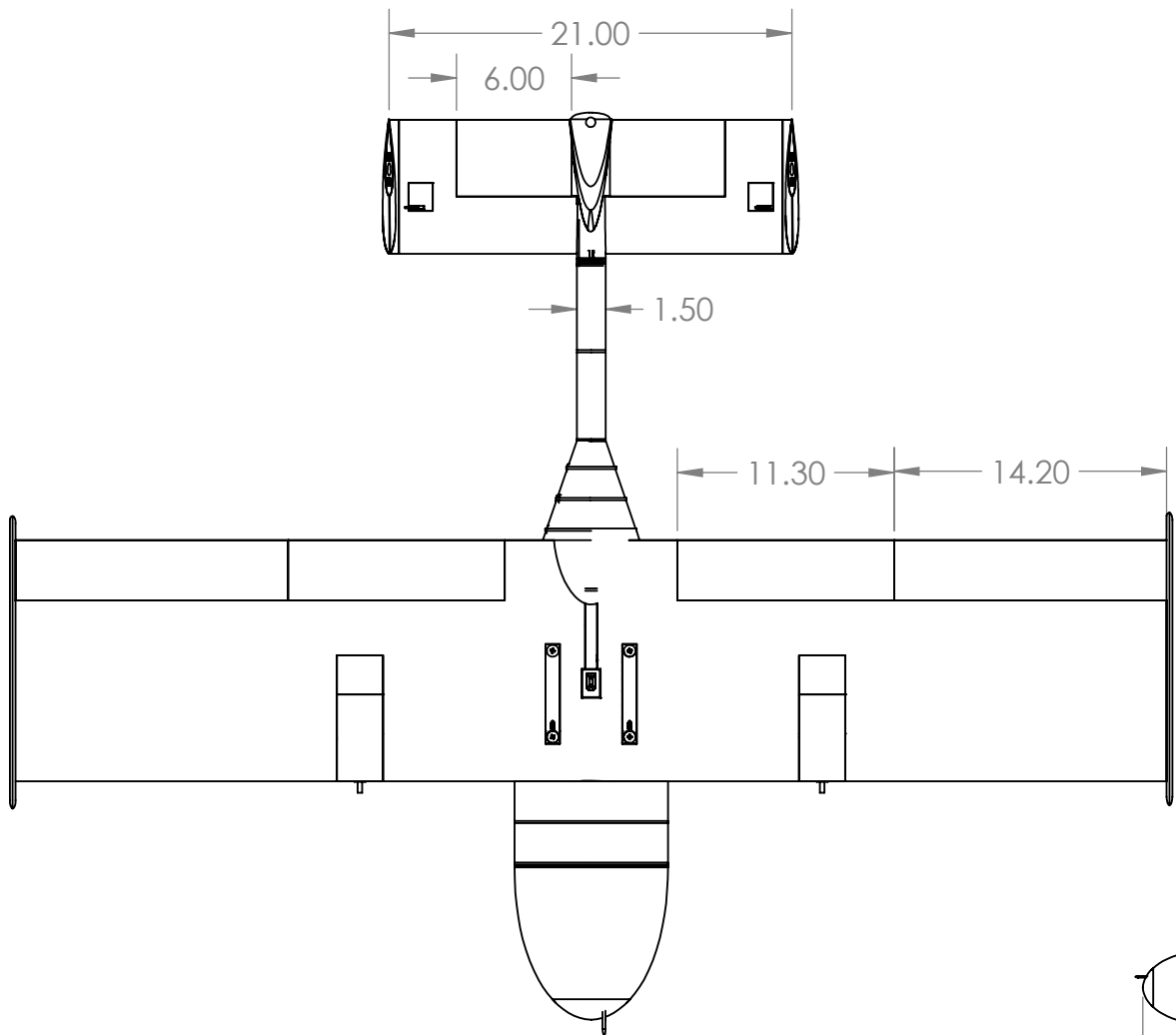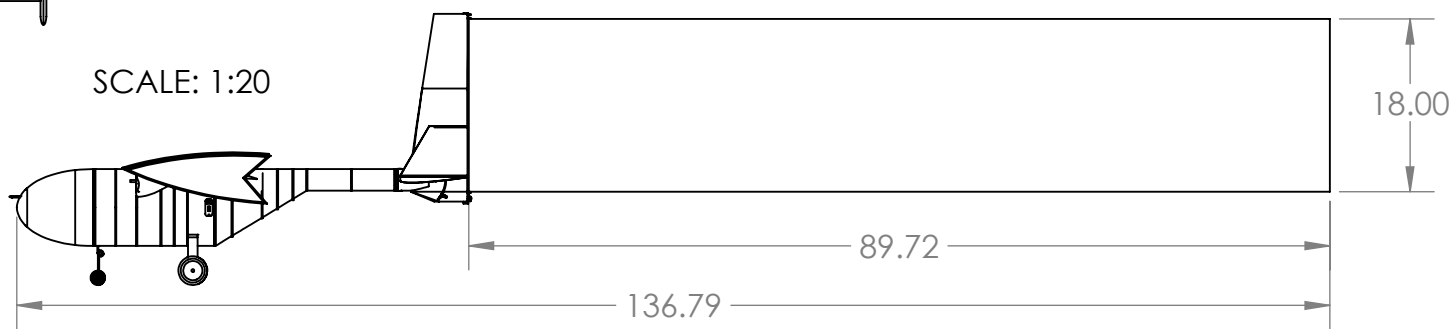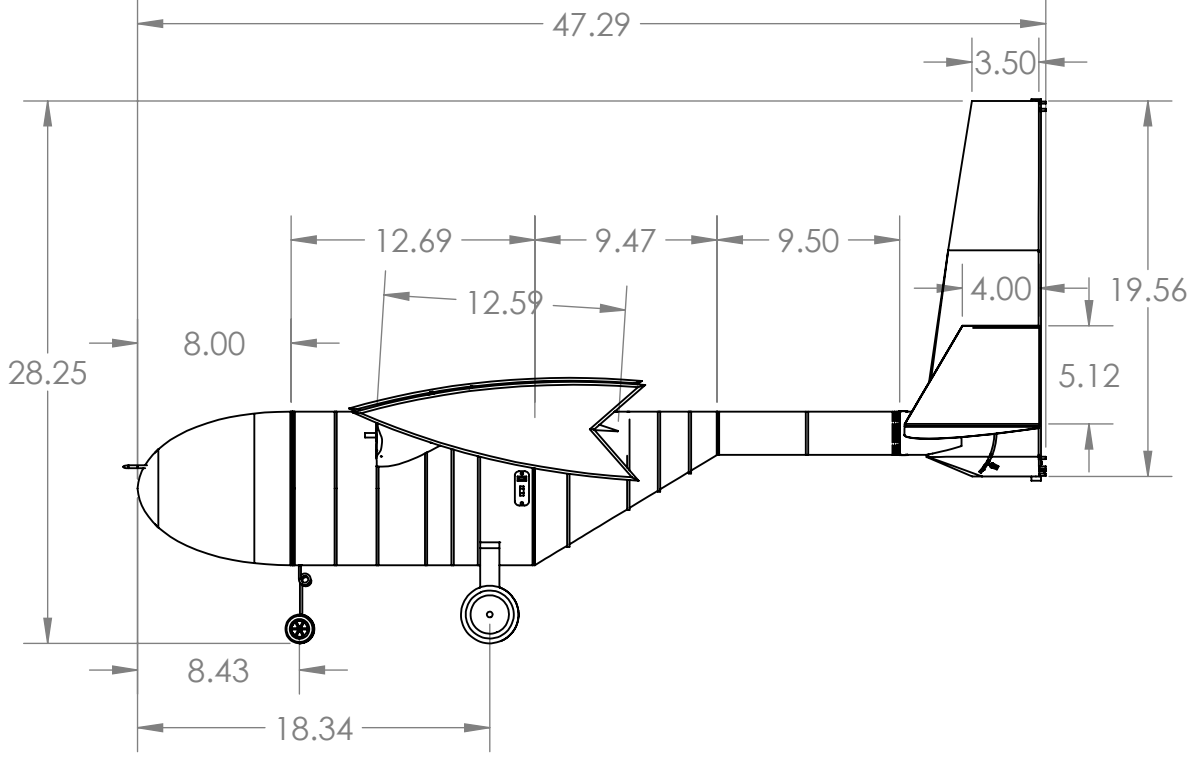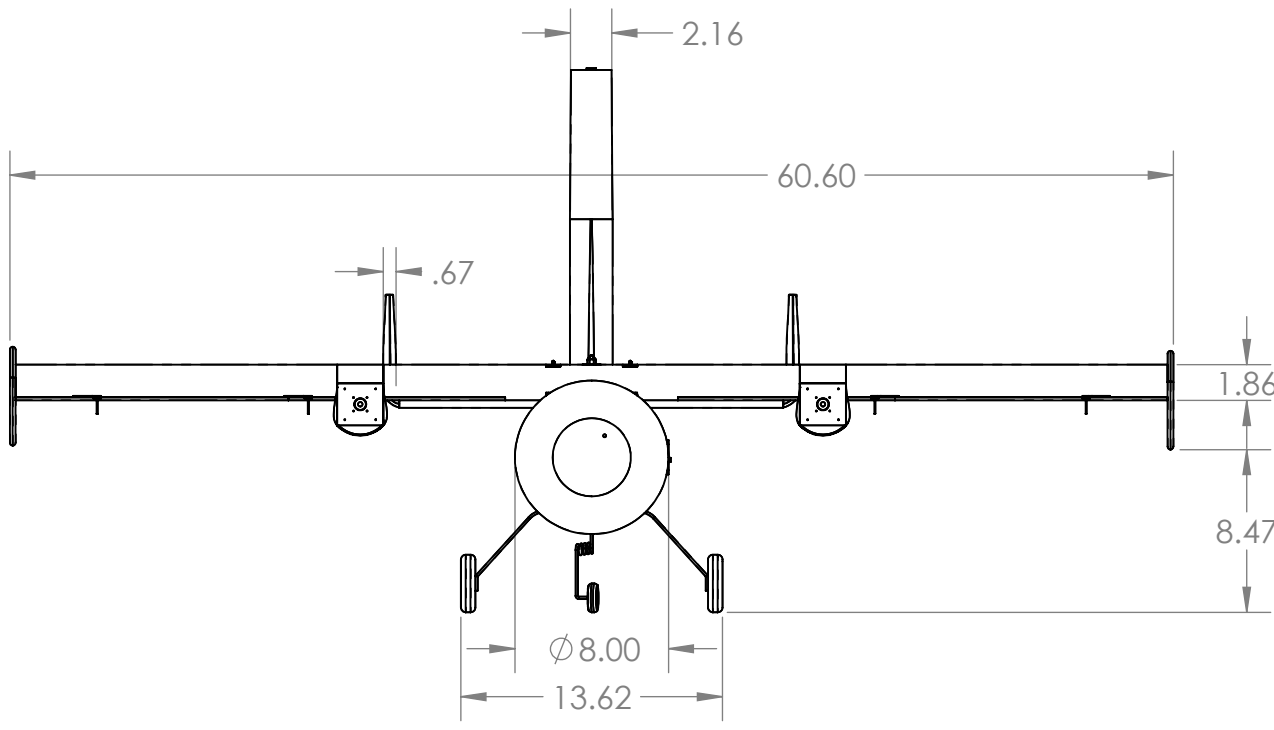
Design, Build, Fly Team
at the University of Washington

TITLE: **Phoenix**

SIZE **B**

Three View

REV

SCALE: 1:10   SHEET 1 OF 1

ITEM NO.	Structure	QTY.
1	Fuselage Frame	1
2	Wing	1
3	Upper Wing-Fuselage Mount	2
4	Lower Wing-Fuselage Mount	1
5	Motor Pylon	2
6	Flap	2
7	Aileron	2
8	Winglet	2
9	Empennage	1
10	Horizontal Stablizer	1
11	Elevator	2
12	Vertical Stablizer and Banner Mechanism	1
13	Rudder	2
14	Empennage Conform	1
15	Nose Cone	1
16	Payload Tray	1
17	Front Landing Gear	1
18	Rear Landing Gear	1
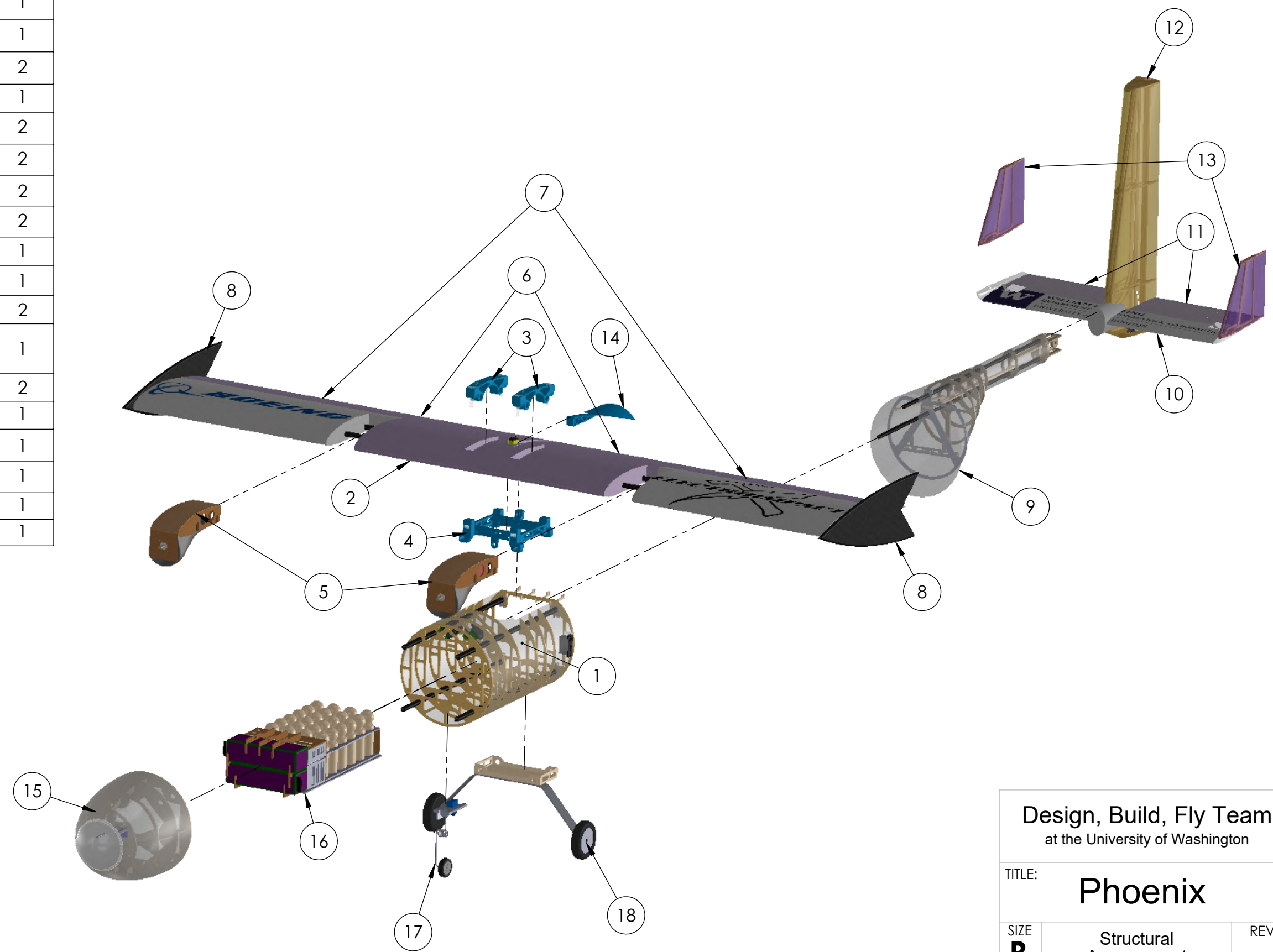
Design, Build, Fly Team
at the University of Washington

TITLE:
Phoenix

SIZE **B**

Structural Arrangement

REV

SCALE: 1:8   SHEET 1 OF 1

| ITEM #	NAME	DESCRIPTION	QTY.
1	Pitot Tube	Hobbypower MPXV7002DP	1
2	Propeller	Config. 1: 15x4 Config. 2: 15x6	2
3	Rx Switch	Futaba Switch Harness	1
4	Fuse/Harness	40A Standard Blade	4
5	Propulsion Battery Mount	Birch Ply Connection to Passenger Tray	1
6	Propulsion Battery	TGY Nano-Tech 4500mAh 6s Lipo	2
7	Rx Battery	TG 1000mAh 2s	2
8	Nose Gear Servo Mount	3D-Printed PLA	1
9	Nose Gear Servo	HXT900 Micro Servo	1
10	Arduino Expansion Board	WYPH Nano I/O Expansion Sensor Shield	1
11	Avionics Chip	Arduino Nano	1
12	Avionics Recorder	Arduino MicroSD Module	1
13	Gyroscope-Accelerometer	MPU6050 Module	1
14	Receiver	TGY iA10B 10CH Reciever	1
15	Elevator Linkage	Steel Rod	1
16	Elevator Servo	HXT900 Micro Servo	1
17	Banner Rod Clasp	Birch Ply	1
18	Banner Servo	HXT900 Micro Servo	1
19	Rudder Ball Linkage	Du-Bro 2-56 Ball Link	4
20	Rudder Servo	TGY Twin BB Digital Micro Servo	2
21	Rudder Servo Mount	3D-Printed PLA	2
22	Arming Plug	XT-90	1
23	Arming Plug Socket	XT-90	1
24	ESC	TGY Plush-32 100A	2
25	Motor	Scorpion SII-4020-630KV	2
26	Flap/Aileron Servo	TGY-50090 M 20T MG	4
27	Control Horn	3D-Printed Plastic	4
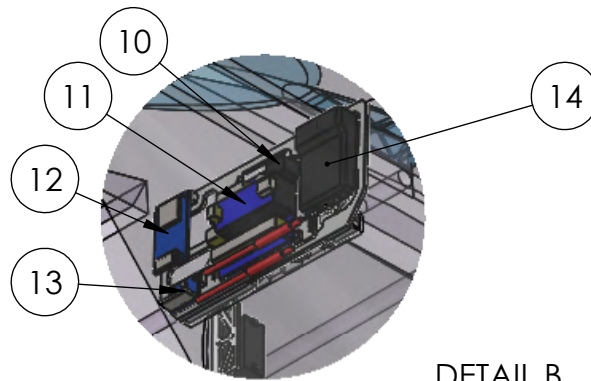
DETAIL B
SCALE 1 : 4
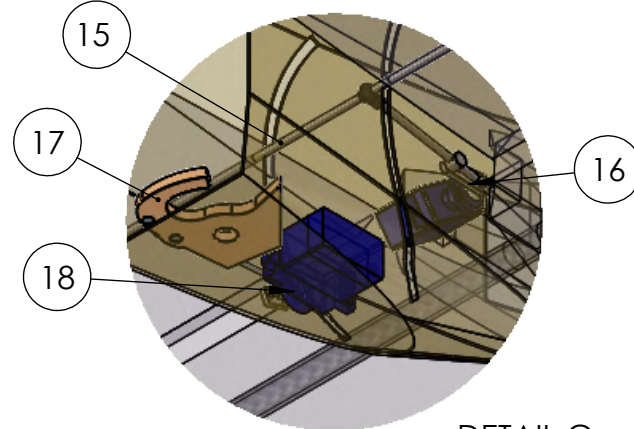
DETAIL C
SCALE 1 : 2
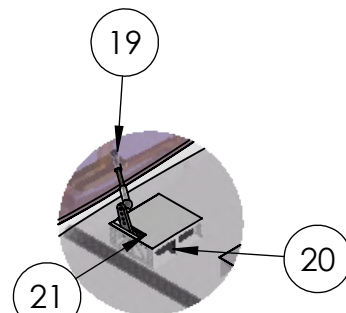
DETAIL A
SCALE 1 : 3
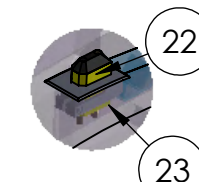
DETAIL D
SCALE 1 : 4

DETAIL E
SCALE 1 : 4
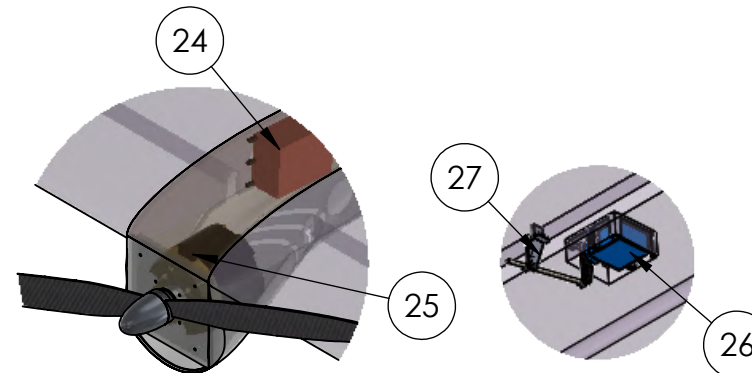
DETAIL F
SCALE 1 : 4
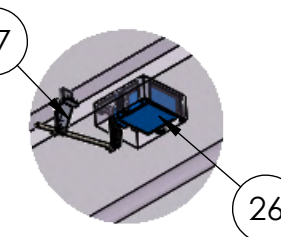
DETAIL G
SCALE 1 : 4
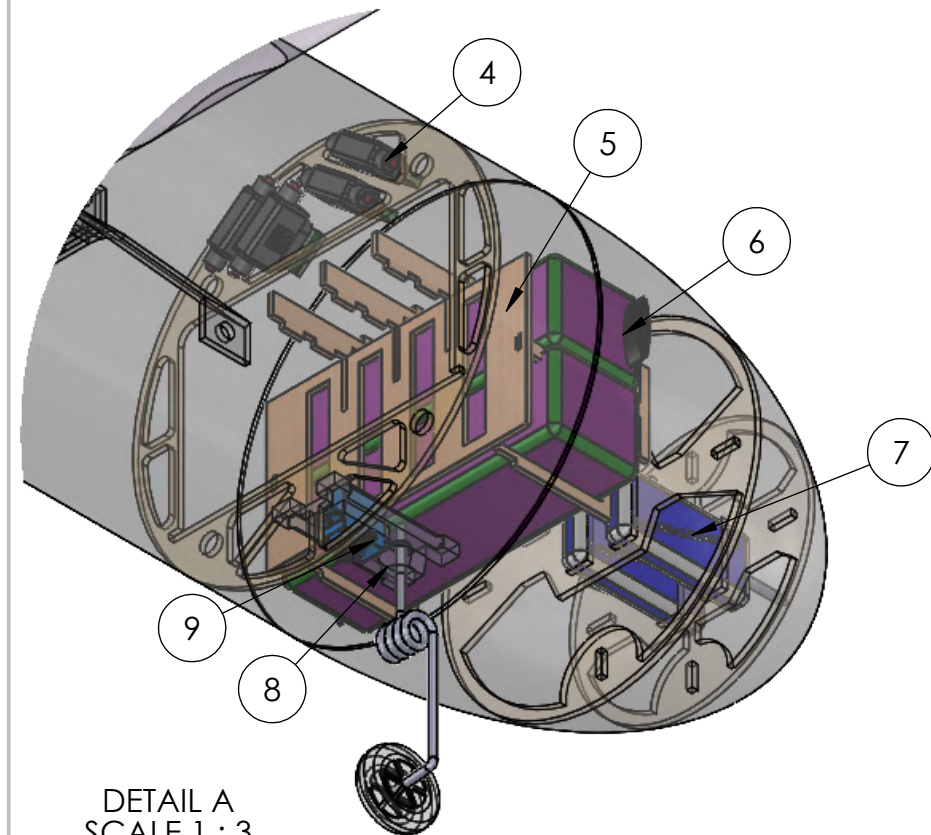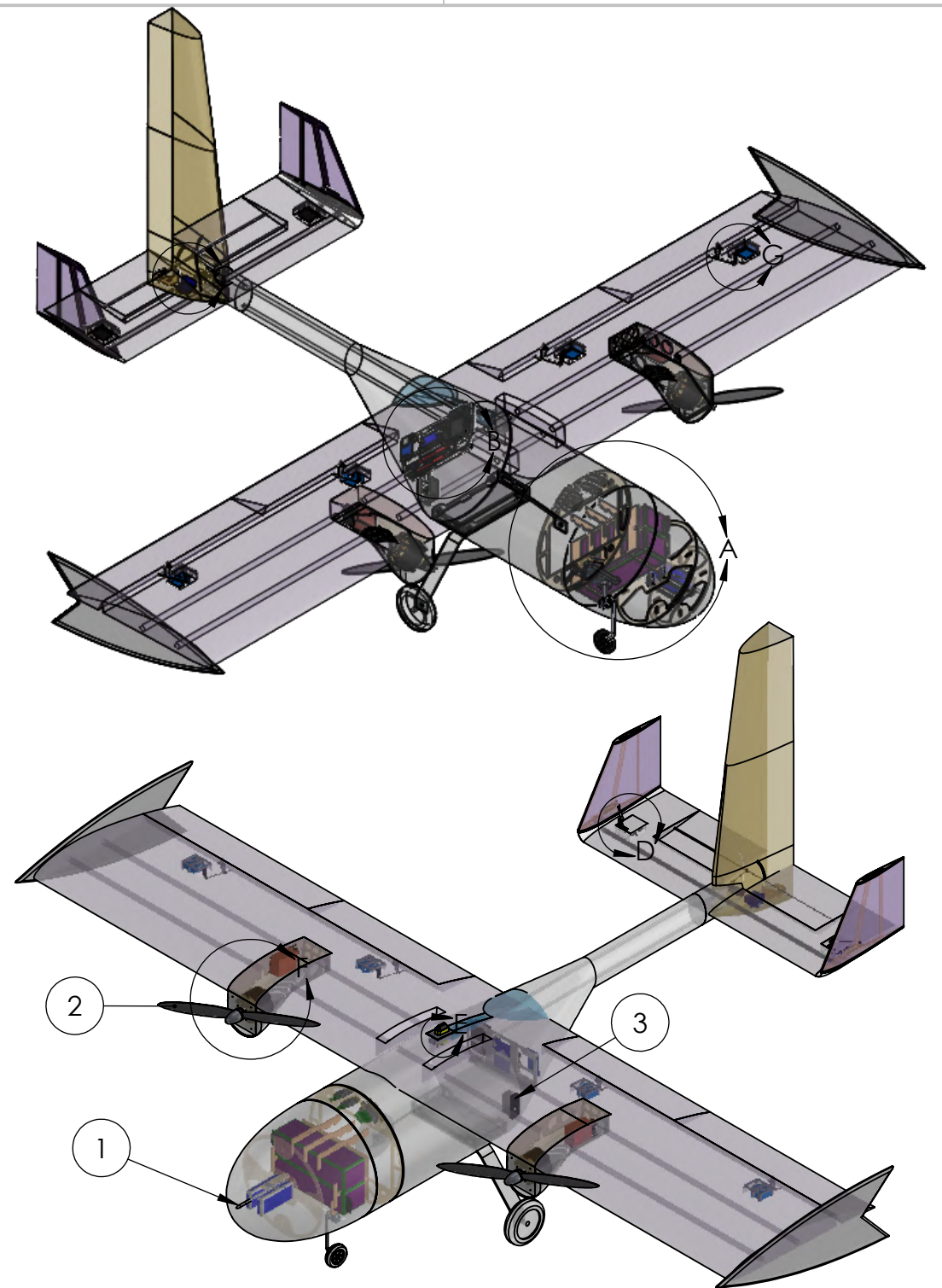
Design, Build, Fly Team
at the University of Washington

TITLE:
Phoenix

SIZE
B

Systems Layout

REV

SCALE: 1:10   SHEET 3 OF 4

ITEM NO.	Component	QTY.
1	Nose Cone	1
2	Fulselage	1
3	Tray	1
4	Tray Roof Structure	1
5	Motor Battery	2
6	Passenger	max 24
7	Luggage	max 24
8	Banner	1
9	Banner Rod	1
10	Banner Deploy-and-Release Servo Mechanism	1

Passenger Tray
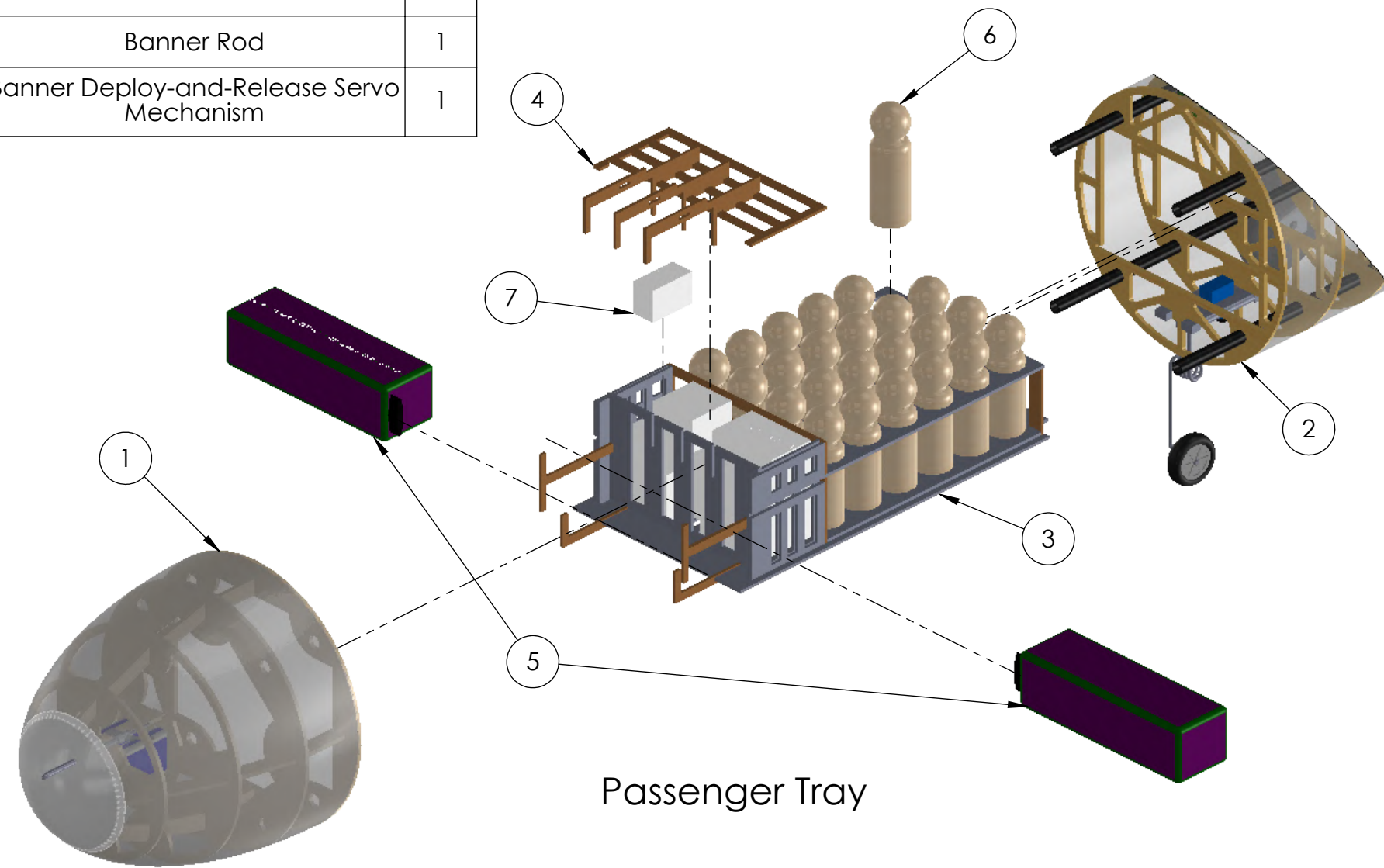
Banner Mechanism
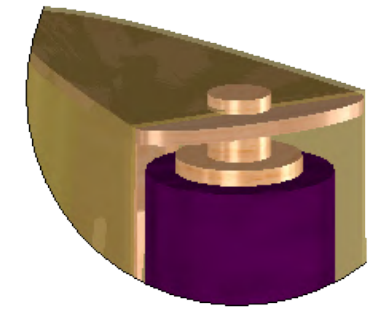
DETAIL B
SCALE 1 : 1.5
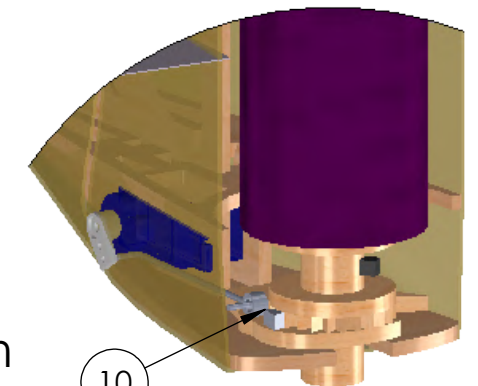
DETAIL A
SCALE 1 : 1.5

Design, Build, Fly Team
at the University of Washington

TITLE:
Phoenix

SIZE **B**

Payload Accommondation

REV

SCALE: 1:4

SHEET 1 OF 1

6. Manufacturing Plan

6.1 Manufacturing Processes Investigated

6.1.1 Equipment and Techniques

Metals: Metals were used because they have a very desirable stress vs strain curve, are very ductile, and have high strength. They have one third the strength to weight ratio compared to composites, but they are far more durable than the quasi-brittle carbon fiber and fiberglass..

Foam Core: XPS foam was found to be very lightweight and flexible, which made it an ideal material for the construction of wing and tail components. It also had the added benefit of being easy to work with and relatively cheap. However, it was known to be unable to sustain large point and distributed loads without reinforcement.

Composites: Composites were known to generally possess high strength to weight ratios and allow for precise manufacturing, which changed the stress-strain performance of the wings. The team investigated balsa wood shells and fiberglass coatings for wing manufacturing but noticed that these methods were more time consuming and less precise.

Covering Film: Covering film, an adhesive shrink wrap, was tacked (glued by heat activation) to a surface or ribbed structure and shrunk tight, smoothing it out. Additionally, it was used to apply compressive stress that resists deformation of the underlying surface. Application of covering film required either a small iron or careful use of a heat gun. The iron was used on covering film for wing surfaces, which caused activation of both the adhesive and shrinkage. However, practice was needed to apply the heat evenly and adjust for heat requirements.

Milling: Milling allowed for the creation of high precision molds and creation of complex shapes. Among the investigations done was the application of high density foam molds to support a pre-preg carbon fiber composite manufacturing process.

3D-Printing: 3D-printing allowed for custom creation of high-fidelity parts. Two primary 3D-printers were used, the Dremel 3D45 and the Stratasys F170. The F170 had a larger build platform and ABS filament capabilities for higher fidelity and stronger structures.

Hot-Wire Cutting: Hot-wire cutting was deemed ideal for cutting out large sections of foam and for the mass production of wing sections. However, this method required a large amount of practice and operator skill for adequate precision. This, combined with the required time to sand down the finished product, made hot-wire cutting a very time-inefficient process. However, training team members to use the cutters during the pre-manufacturing phase increased efficiency greatly, and running two hot-wire cutters in tandem further improved efficiency.

Laser Cutting: Laser cutting was useful for parts that require a high degree of precision and was most preferable for birch wood cutting. While the CAD process was slightly time consuming, the process remained quite time efficient, with cut times averaging anywhere between 5-10 minutes. This method was used to cut out birchwood stencils to guide hot-wire cutting for wings, and for the creation of ribbed wing parts.

6.2 Material Selection

A materials research team investigated materials and manufacturing processes and weighed them against five factors in order to decide what processes and materials were best.

Factor	Assigned importance
Cost	3
Manufacturing Speed	2
Strength	4
Weight	4
Difficulty of fabrication	2

Table 6.1: Material selection priorities

Cost: While quality was the main priority, the limited budget curtailed the ability to use the best resources and methods of fabrication.

Speed of Manufacturing: Given that a significant amount of parts had to be manufactured multiple times, the team could not afford to spend an extended period of time fabricating a single piece as that would slow down the entire tandem assembly process.

Strength: The structural integrity of the aircraft was the highest concern for the team since the design parameters stipulated that the configuration would undergo variable loading between missions. Additionally, any deformation in materials increased the risk of fatigue failure.

Weight: While strength was a large factor, weight had to be considered. In order to carry more passenger loads, the structural weight had to be minimized.

Difficulty of fabrication: The difficulty of the fabrication techniques were also considered, since the majority of the team was composed of first year students.

Tables 6.2 and 6.3 detail the analysis and scoring of materials and manufacturing methods investigated. The two largest constraints were difficulty of fabrication and cost.

Manufacturing technique comparison					
	Factor	Hot-wire cutting	3D-Printing	Laser cutting	Milling
Cost	3	5	4	5	2
Manufacturing speed	2	3	2	5	2
Difficulty of fabrication	2	4	4	5	1
Total		**29**	**24**	**35**	**12**

Table 6.2: Comparison and scoring of manufacturing techniques

Material comparison					
	Factor	Metals	Foam core	Composites	Covering film
Cost	3	3	5	2	5
Manufacturing speed	2	2	4	2	3
Strength	4	5	1	5	1
Weight	4	1	4	3	4
Difficulty of fabrication	2	3	4	2	3
Total:		**43**	**51**	**44**	**47**

Table 6.3: Comparison and scoring of characteristics of materials

Part	Manufacturing Technique
Wings	Hot wire cutting, laser cutting, composite, 3D printing, foam cores
Fuselage	Laser cutting, composites, foam cores (mould)
Landing gear	Metals, laser cutting, 3D printing
Tail	Hot-wire cutting, laser cutting, composite, 3D printing, foam cores, covering film
Banner	Laser cutting, 3D printing
Nose cone	Laser cutting, 3D printing, composite, covering film

Table 6.4: Manufacturing techniques required for each component

6.3 Major Component Manufacturing Process

6.3.1 Wings

A rectangular piece of XPS foam was cut to the length and width of the selected airfoil, a NACA 4412. Laser-cut stencils of the airfoil were glued onto each side of the foam and a hot-wire cutter, operated by two individuals, was used to cut the foam to the desired shape. The foam sections were sanded smooth, while control flaps were cut from appropriate sections. The control flaps were then reattached with woven aramid fibers and epoxy resin to create a seamless, flexible hinge. The purpose of the aramid hinge was to reduce skin friction on the control surfaces, which preserved laminar flow. Additionally, a premade fiberglass sheet was placed over the ailerons to create a smooth surface for the same reason. The wing sections were assembled with 2 carbon fiber spars running along the length of the wing to increase stiffness and reduce deflections. A layer of balsa wood was applied using Super M 77 spray adhesive. The balsa was then sanded smooth, then layed with a continuous sheet of 2.6 oz. per sq. yd. fiberglass.

6.3.2 Fuselage

In order to create a fiberglass skin for the fuselage, a foam cylinder with the same dimensions as the final fuselage was laser cut from XPS foam to create a positive mold. Fiber glass was then wet-laid over the surface between two sheets of mylar release film to form a skin. Wood stencils of the ribs were laser cut and attached to carbon fiber spars with epoxy to make the internal structure of the fuselage. After wire insertion, the fiberglass skin was set to the ribs with slow cure epoxy.

6.3.3 Landing Gear

A strain-hardened 0.125 in thick aluminum bar was used to form the main landing gear, and 4 mm diameter hardened stainless steel wire was used for the steerable nose gear. Main landing gear wheels were 3 in rubber wheels, and the nose wheel was a 2.5 in foam wheel. The main landing gear mount was made of 0.125 in laser cut birch plywood set with epoxy to ribs and lower spars in the fuselage and the aluminum bar was then screwed onto the mount. The nose gear used a 3D-printed mount which was designed to mount onto special cutouts in the ribbing.

6.3.4 Tail and Banner

The horizontal stabilizer was constructed similarly to the wing, where a XPS foam core was cut with a hot-wire cutter, which then had balsa wood and fiberglass skin added to it, with a 8mm carbon fiber rod composing the main axial support. The elevators were attached with an aramid hinge and were linked through a steel control rod. The vertical stabilizer and rudders were made out of 0.125 in laser-cut plywood. These then had covering film applied to them to make them streamlined. The connection between the horizontal stabilizer and the rudders was a PLA 3D-printed piece that was epoxied onto the structure. The rudder servos were secured in place with PLA 3D-printed brackets, while the elevator and banner release mechanism servos were secured in the wooden frame of the vertical stabilizer.

The banner release mechanism had a 19.875 in long 0.5 in wood dowel at its core, with 0.125 in plywood laser cut circles of 1.5 in diameter, a circle of 1.0 in and a tooth gear all super-glued to a wooden dowel. The lock that interfaced with the tooth, connection point for the servo linkage, and the pivot point for the locking mechanism were all PLA 3D-printed parts. The locking mechanism was made out of the same 0.125 in plywood.

6.3.5 Motor Mount

In order to save weight and costs, the mount's structural material consisted of 0.125 in thick birch plywood. The mounts were cut using a laser cutter, with the design of the mount including many weight saving holes made throughout the structure. The mount also had a skin consisting of 1/32 inch thick balsa wood, which would make it easier to flawlessly integrate into the wing. The different laser cut sections of the mount were bonded together with quick-drying epoxy for ease of manufacturing, as well as considerable durability. The motor mount was designed to directly mount to the wing's carbon fiber spars within pre-cut sections of the wing for ease of installation.

6.3.6 Passenger Tray

Over time, the CAD designs were decomposed into flat, individual components that could be laser cut precisely out of balsa wood. Each piece of the passenger tray was cut from balsa wood and assembled using epoxy, which gave the tray a significant structural strength to weight ratio. After assembly, the sides and faces of the tray were sanded down to ensure smooth sliding between the slots cut into ribs that would hold the tray.

6.3.7 Nose Cone
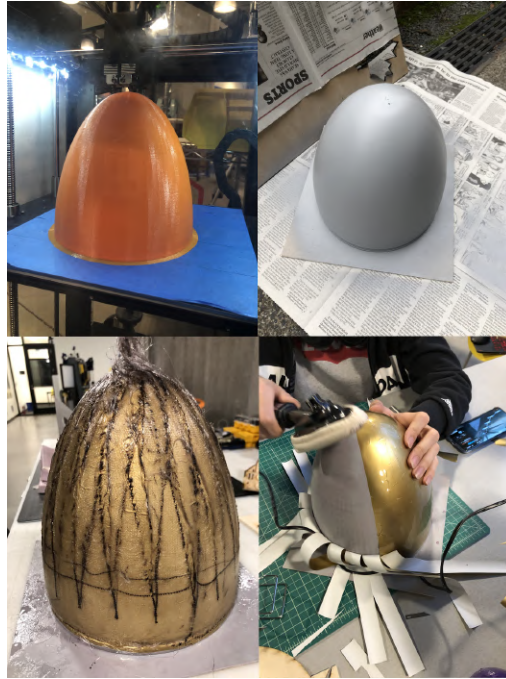
Figure 6.1: (Clockwise from top left): 1. Mold being 3D-Printed, 2. Primed and sanded, 3. Release film applied, 4. Fiberglass layup

To construct the positive nose cone mold, the nose cone model was hollow 3D-printed on a large format printer. The mold was then sanded smooth with fine 400 grit sandpaper and spray-painted with primer. There were multiple rounds of sanding and spraying to create the finished mold. A gel coat release was evenly applied onto the mold, then fitted with a release film over the mold surface. An acrylic stencil for the second shape of the nose was then made. Strips of fiberglass were used to make the composite layup. Two additional overlapping fiberglass layups were then applied. After curing, the nose cone was sanded and cut into three pieces.

The four ribs of the nose cone were laser cut and assembled using epoxy to hold everything together. The structure behind the tip of the nose cone was 3D-printed to accommodate the pitot tube. The edge of each rib was sanded to allow for maximum contact with the fiberglass pieces which were laid up over the ribs. Lastly a thin strip of fiberglass was laid up over the seams of the fiberglass pieces and sanded.

6.4 Manufacturing Schedule

	Date	11/2/19	11/9/19	11/16/19	11/23/19	11/30/19	12/7/19	1/4/19	1/11/19	1/18/19	1/25/19	2/1/19	2/8/19	2/15/19	2/22/19	2/29/19	3/7/19	3/14/19	3/21/19	3/28/19	4/4/19	4/11/19	4/18/19
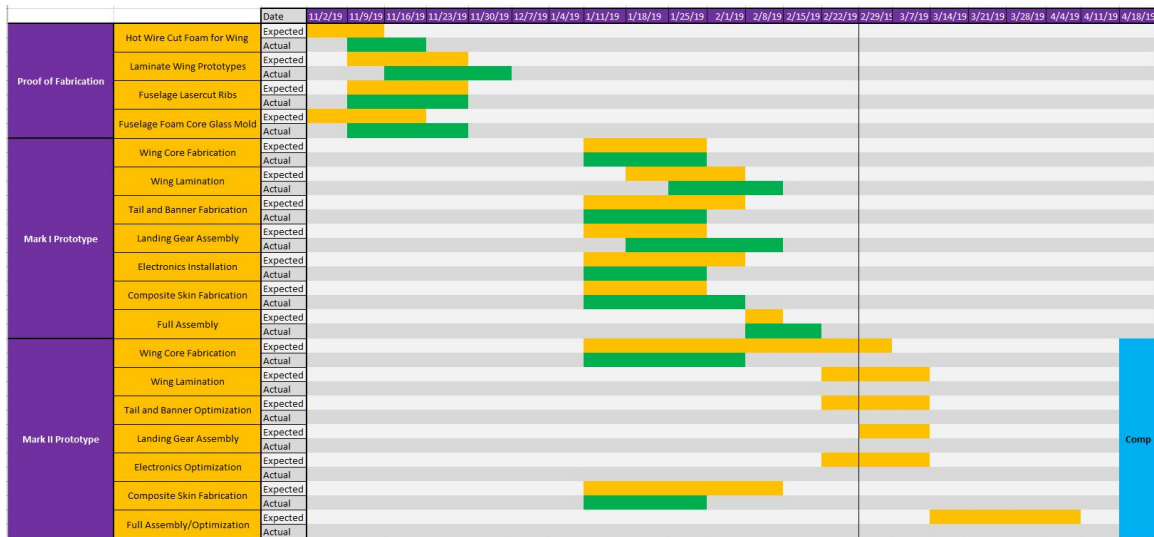
Table 6.5: Manufacturing Schedule

7. Testing Plan

7.1 Subsystem Test

7.1.1 Battery Test

Main battery testing consisted of 2 tests, loading the chosen TGY 4500mAh Nano-Tech battery and loading of a 4500mAh DJI Smart Battery through static testing with one of the flight motors. Testing consisted of running the motor at throttle settings consistent with a simulated flight and monitoring supplied current and power until the battery voltage reached a lower limit of 21.5 V. The test evaluated both flight time potential and battery power deliverance capacity. Static testing was also completed for potential batteries at the beginning of the manufacturing phase.

7.1.2 Banner Test

Due to the lack of literature found on banner drag, it was decided to conduct testing using a mount attached in the bed of a pickup truck which would drive up to 50 mph so that airspeed and force measurements were able to be taken. In order to measure drag force from the banner during simulated flight, a low-friction rail system was used, which held a lightweight 1.95 lb banner mount mechanism. The force exerted on the mechanism was fed directly into the force

gauge suspended between the mount and air gap. This allowed for an accurate measurement, provided the friction force was taken into consideration.

A testing system was created that combined visual data with measured data in order to have a system for result validation. In order to capture visual data, an FPV camera was mounted directly below the banner which shows flutter characteristics in the z-axis (vertical with respect to the Earth.) A chase car was also implemented to evaluate flutter characteristics in the y-z plane.

Figure 7.1: Banner testing structure

There were 7 tests conducted with this system, testing 3 different types of materials: an uncoated nylon banner, silicone and polyurethane coated nylon, and a higher denier coated diamond weave nylon. All test banners were based on a 1 ft by 5 ft size, except for one smaller banner which was 6 in by 3 ft.

When tests were performed with towlines, the banner did not stay vertical, so that method of attaching the banner to the plane was rejected. The silicone and polyurethane-coated (impregnated) nylon was determined to be the best choice for material as it frayed the least and had the lowest drag at higher airspeeds. The uncoated nylon was similar in drag, but it frayed far more than the impregnated nylon, so the impregnated nylon was chosen. A folded banner that would have allowed for a larger banner to be mounted to the same fixed deployment rod was tested, but it was ultimately rejected due to a lack of vertical stability and excessive complexity.

7.1.3 Structure Test

It was determined that a cantilever beam test would effectively simulate the loading conditions experienced by a wing in flight. This was made under the assumption that if an airfoil can resist a point load at the tip, it can resist the same distributed load across the entire surface. For the test, 6 in of the airfoil were clamped onto a table to simulate the fixed fuselage mount and suspended the other 18 in out over the edge for point load application. In order for the test to be successful, the airfoil had to be completely rigid at the fixed end, resulting in the design and manufacture of the larger clamping mechanism. Additionally, in order to protect the fragile trailing edge of the airfoil, another clamp was designed which was mounted on the free end of the airfoil and acted as the center for the point load application.

To simplify testing, the load was applied in increments of 0.5, 1.0, or 2.0 kg, depending on the predicted strength of the airfoil. At each loading increment, the angle of deformation and the surface deformation were measured to determine the stiffness of the airfoil. Conductive paint was applied to the top and bottom surfaces of the airfoils and the resistance across the paint was measured to calculate the change in length as the airfoil surface deformed.
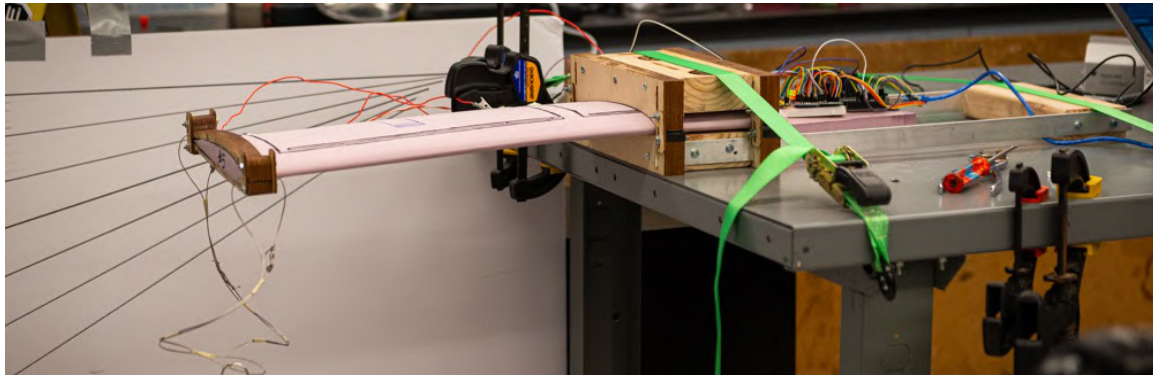
Figure 7.2: Static wing loading mechanism

7.1.4 Propulsion System Test

The full propulsion system, which included the control system and associated electronics, was tested during the manufacturing phase. A static test mount made from wood was developed from the repurposed banner test mount. The static motor test mount was capable of holding a single motor and the corresponding electronic components. A force sensor was used to determine the thrust generated by the motor, while the control system recorded the voltage and amperage of the battery as the motor was running.

7.2 Flight Test

7.2.1 Flight Mission Simulation

During the design and build process, an accurate model of the aircraft was kept updated in RealFlight 8, a remote control simulation program. This software approximated the performance characteristics of the aircraft and allowed pilots to become familiar with predicted aircraft handling characteristics. While it was not possible to simulate a banner, loaded and unloaded missions were flown and landings were extensively practiced to ensure the aircraft could be landed with minimal risk of damage to the airframe.

7.2.2 Test Flights

Nose wheel steering was confirmed to perform as expected while the aircraft rolled under its own power. Differential thrust from the wing-mounted motors supplemented the nosewheel steering and allowed the aircraft to turn sharply while taxiing. Once the aircraft was confirmed to be stable on the ground, the flight phase of testing could begin. An initial proof of concept flight was conducted to verify the aircraft's airworthiness and become familiar with the aircraft's handling characteristics. Maximum performance maneuvers were not attempted during this flight. Once the aircraft has been trimmed and modified according to the flight observations, further flight tests will be performed to confirm various mission capabilities. The small 1 ft x 5 ft banner will be deployed and released, then replaced by the large 1.5 ft x 7 ft banner and the behavior of the aircraft observed. Takeoff distance will be demonstrated to be less than 20 ft with the largest banner installed. First half of passenger capacity will be loaded, and once satisfactory performance has been demonstrated, the aircraft will be loaded to maximum passenger capacity and flown at its maximum weight. Further flights will fly a mock test course and be timed to predict competition score and refine flying technique.

7.2.3 Flight Log

Design, Build, Fly at the University of Washington Flight Log

Note: Please upload this flight log to the online folder pertaining to the corresponding aircraft.

Flight #: _____   Take-Off Time: _____ AM / PM
Date of Flight: _____/_____/_____   Flight Duration: _____ Min _____ Sec
Battery Used: _____   CG Location: _____
Total Takeoff Weight: _____ lb.   Weather: _____
Wind Conditions: _____ mph, coming in from N / NE / E / SE / S / SW / W / NW

Pre-Flight Checklist:
- Motor securely fastened
- Wing securely fastened
- Empennage securely fastened
- Landing gear lubricated and rolling smoothly
- Payload onboard and secured
- Main battery connected
- Propeller free of obstructions
- Power on
- Full control surface deflection
- Full motor speed control

Post-Flight Checklist:
- Power off
- Main battery disconnected
- Aircraft inspected for damage

Purpose of Flight:
_____
_____
_____

Payload:
_____
_____
_____

Notes:
_____
_____
_____
_____
_____

Figure 7.3: Flight log format

7.3 Testing Schedule

Date	Objective
2/18/20 (First Flight)	Smooth takeoff, trim aircraft for stable flight, evaluate handling in climbs, descents, left and right banks, perform practice approach to landing surface, land aircraft.
3/21/20 (Banner Testing)	Load aircraft with 1 ft x 5 ft banner, confirm 20 ft takeoff, test banner deployment, effects on handling, and release. Repeat with 1.5 ft x 7 ft.
3/22/20 (Passenger Testing)	Load aircraft to half passenger capacity (12 passengers) and evaluate aircraft handling. Repeat with maximum (24) passenger load.
3/23/20 - 4/1/20 (Mission Practice)	Fly simulated and timed mission course to refine pilot technique and optimize aircraft performance.

Table 7.1: Major flight test dates and objectives

8. Performance Results

8.1 Subsystem Test Results

8.1.1 Main Battery Test

It was determined, through simulation of flight cruise conditions, (with periodic variation), that each main propulsion battery option has sufficient capacity to provide an average of 40 Amps of current to each motor for the necessary maximum 12-13 minute flight time. Testing additionally revealed a peak current provision of 72 Amps, providing the basis for choosing a total of 80 Amps in fuses and 80+ Amp ESCs.

8.1.2 Propulsion System Test

Testing of the propulsion system successfully verified the capabilities of the selected Scorpion motors. Testing revealed that at simulated cruise conditions of 50% throttle, each motor provided approximately 12 lb of thrust, equivalent to the predicted cruise requirements. Testing additionally proved a peak trust of approximately 22 lb of thrust at full throttle.

8.1.3 Structure Test

Primary considerations in the selection of a wing material included ease of manufacturing, weight, strength, maximum sustainable deformation, reusability with minor deformation, and repairability of damage. Reduced weight and deformation, as well as increased strength, optimized aircraft performance within the flight envelope. Increased reusability, repairability, and ease of manufacturing reduced manufacturing time and overall cost.

|	Type of Manufacturing	Airfoil weight analysis		
		XPS Core (grams)	Final weight (grams)	% mass increase
1	Control (just XPS)	49	49	0%
2	XPS, Balsa	52	96	85%
3	XPS, Balsa + LE fiber cloth	54	126	133%
4	XPS, Balsa + Full fiber cloth	49	136	178%
5	XPS, Full fiber cloth (1 layer)	50	83	66%
6	XPS, Full fiber mat	47	200	326%
7	Birch Ribbed, Covering Film	94	107	N/A

Table 8.1: Wing weight analysis
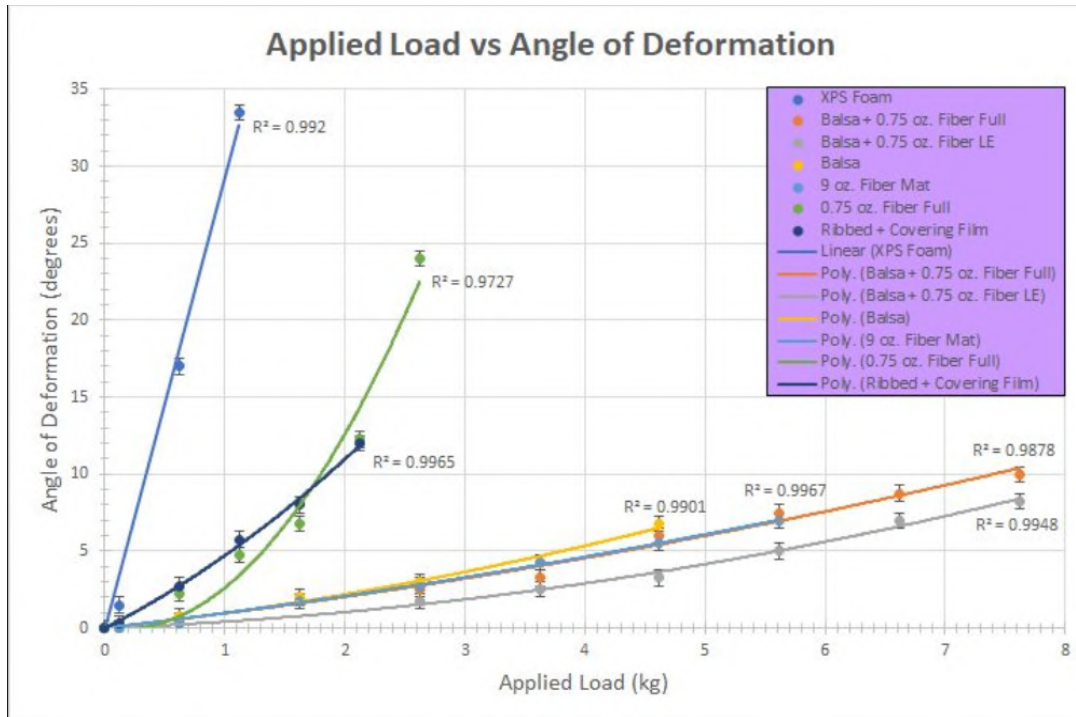
Figure 8.1: Wing material loading under various loads

The above graph represents the behavior of all tested airfoils under a point load application, as described in section 7.1.3. The stiffest materials were shown to be all the balsa wood and fiberglass mat composites, while the ribbed and fiberglass cloth were shown to be substantially more ductile.

Following banner testing, the drag of each material was graphed against the corresponding airspeeds.
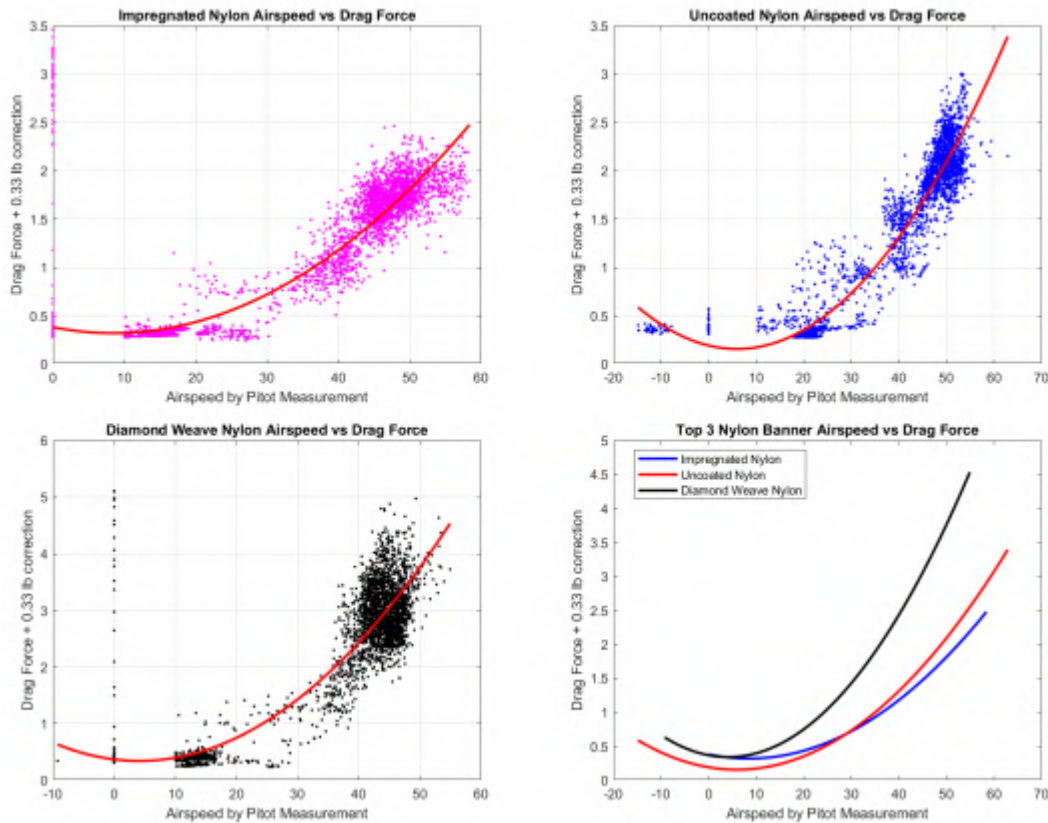

Figure 8.2: Banner drag test results

Based on these graphs, it was concluded that the impregnated nylon not only outperformed both the uncoated and diamond weave materials in high speed drag, but it also had a lower peak value. Thus, it was determined to be the most optimal material. Furthermore, upon investigation of the material post-test, the impregnated nylon was the most durable and sustained the least amount of damage throughout two uses. The uncoated nylon was second in durability and the diamond weave came in last. Only three materials were analyzed by graphing due to the observation that the towline banner did not maintain orientation and would not be an effective way to manufacture the banner. A possible solution would have been to reinforce the leading edge of the banner (plane side) with a sturdy rod to mimic the support of the fixed support test. While

theoretically towlines could have been used to support the banner, it was ultimately determined that using a fixed rod provided the highest reliability in keeping the banner orientation fully vertical.

A banner with the same aspect ratio and ¼ the total area was also tested. This revealed a drag value of about half that of the larger banner, suggesting that banner drag was proportional to the length of the banner rather than the area. This led to the conclusion that larger banners were able to be utilized and still have lower drag values than those predicted by literature. From these numbers, a drag of about 3 Newtons was generated by the impregnated nylon 1 ft by 5 ft banner, and a drag of 4.5 Newtons was generated by a 1.5 ft by 7.5 ft banner. Compared to approximations of towable banners in literature, drag was substantially less, which provided confidence in the upscaling of the banner. This may have been a result of the banner being fixed to a rod rather than a towline.

8.2 Flight and Mission Performance

8.2.1 First Flight Test - Outcome

Once systems checks were complete and all trims were set to neutral, the aircraft was moved to the end of the runway surface. Throttle was smoothly advanced to about 80% with elevator back-pressure until rotation occurred and the aircraft became airborne. Ground roll was qualitatively observed to be shorter than expected. After takeoff, the nose pitched up into a steep climb and full forward elevator was insufficient to recover from the climb until heavy nose-down trim was applied. Available power was sufficient to hold the aircraft in the climb. In flight, the aircraft tended to quickly pitch into a climb with neutral controls, even after trim was applied. The strong pitch-up tendency of the aircraft required constant forward elevator input and made it extremely difficult to keep sufficient airspeed to maintain stable flight. Roll control was extremely sensitive and aggravated the pitch instability even further. These handling issues eventually compounded to cause catastrophic loss of control and a spiral into the ground.

Figure 8.3: Inflight photo during the flight test campaign

8.2.3 Confirmed Performance

Takeoff distance was observed to be satisfactory, and engine power was well in excess of what was needed for this unloaded aircraft, but that extra power will be needed to overcome the drag of the banner. Aircraft structure held up well even in demanding maneuvers like vertical climb and a spiral. The flight control electronics worked as expected.

8.2.4 Accident Analysis and Recommendations

Post-flight analysis of the horizontal stabilizer revealed that the design angle of incidence of -3 degrees was increased to -5 degrees by manufacturing error and that the drag moment from the tall vertical banner mount was not taken into account when setting the horizontal stabilizer. Changing the simulated model to match the actual tail was able to recreate the runaway pitch condition in RealFlight 8. Aileron travel was also deemed dangerously large, making smooth turns difficult and possibly inducing tip stalls at full deflection.

Changes were made to address the discoveries from the accident. The horizontal stabilizer angle was reduced to -1 degree and the elevator trimmed down. Aileron travel was reduced and a switch to toggle between high and low dual rates for the ailerons was added.

9. References

[1] "2019-20 DBF rules", AIAA [online], http://www.aiaadbf.org/Rules/.

[2] Raymer, Daniel P. "Aircraft design: a conceptual approach - 6th edition", AIAA, 2018.

[3]"Aerospaceweb.org | ask us - rocket nose cones and altitude ." Aerospaceweb.org [online]. http://www.aerospaceweb.org/question/aerodynamics/q0151.shtml

[4] "How to read an RC receiver with a microcontroller", RCArduino [online], http://rcarduino. blogspot.com/2012/01/how-to-read-rc-receiver-with.html

[5] "Performance data", APC [online], https://www.apcprop.com/technical-information/ performance-data/

[6] Hoerner, S. "Fluid-Dynamic drag", Hoerner Fluid Dynamics, New York. 1965.